Elena Gianina Frimu
Master Nanotech

Master Thesis

Model based design and validation of a mixed signal integrated circuit

February 14, 2022 - August 12, 2022

Supervised by

- **Company supervisor:** Benjamin Colle - *bco@melexis.com*
- **School tutor:** Dr. Laurent Fesquet - *laurent.fesquet@univ-grenoble-alpes.fr*

Confidentiality: NO

École nationale supérieure de physique, électronique, matériaux - Phelma
Bât. Grenoble INP - Minatec
3 Parvis Louis Néel - CS 50257
F-38016 Grenoble Cedex 01
Tél +33 (0)4 56 52 91 00
Fax +33 (0)4 56 52 91 03
http://phelma.grenoble-inp.fr

Melexis Technologies
Chemin de Buchaux 38
2022 Bevaix - Suisse
Tél +41 32 847 06 60
https://www.melexis.com

Acknowledgments

First and foremost, I would like to express my gratitude to Benjamin Colle and Zsombor Lázár for giving me the opportunity to work on such an interesting project. I would like to thank them and the other members of the THIL team, Jeroen Rits, Martin Savary and Oleksandr Zhuk, for their trust, patience, caring and encouragements. They always found time to answer my many questions and help me find solutions to the problems I encountered. It was a great pleasure to work with them and learn from their valuable experience.

My sincere thanks go to Jérémie Chabloz and Gilles Curchod who often took time out of their busy schedule to answer the questions I had on the MLX90427.

More generally, I would like to thank all the colleagues from Melexis for their warm hospitality.

I am also very grateful for the valuable guidance and feedback I received hthroughout this internship from my school tutor, Laurent Fesquet. His advice allowed me to share my results in a clear and efficient manner.

Last but not least, I would like to express my special thanks to the other interns, Cristiano Merio, Titouan Matheret, Tim Bürgel and Syrine Mansour, for the ping pong games at lunch and for the good company over the last six months.

Contents

Acronyms

ADC Analog-to-Digital Converter. vii, 6, 9, 10, 16–18, 20, 21

AFE Analog Front-End. iii, viii, 1, 6, 9, 12–14, 16, 18, 19, 32–34

ASIL Automotive Safety Integrity Level. 6, 23, 25

CI Continuous Integration. 29, 30, 32–34

CPU Central Processing Unit. 6

DMA Direct Memory Access. 10, 18

DUT Device Under Test. 12–14

ECU Electronic Control Unit. 26

ESP Electronic Stability Program. 6

FDS Full Diagnostic Sequence. 9, 21

FPGA Field Programmable Gate Array. 12–14

HIL Hardware-In-the-Loop. 1, 11–13, 25

IMC Integrated Magnetic Concentrator. 3–7, 16

MUPET Melexis Universal Program and Test. 6

NVRAM Non-Volatile Random-Access Memory. 7, 9, 10, 13, 19, 32

RAM Random-Access Memory. 16

ROM Read-Only Memory. 7, 10, 11, 18

SPI Serial Peripheral Interface. 6, 9, 13, 14, 29, 32

SRAM Static Random-Access Memory. 7

SWCC Software Competency Center. 30, 32

THIL Triaxis-Hardware-In-the-Loop. viii, 2, 12–15, 28, 30–34

TPMS Tire Pressure Monitoring Systems. 1

List of Figures

1 Introduction

System-level testing is one of the most expensive steps when developing a product with embedded computing. As the software complexity of modern products is increasing, minimizing the time-to-market, while thoroughly testing any significant change, is becoming ever more challenging. This is especially the case in the automotive industry, where smart sensors are more and more involved in safety-critical functions. Hardware-In-the-Loop simulation is commonly employed for the testing of complex real-time embedded systems, as it allows increasing the test coverage in a fast, affordable, reliable and repeatable manner. During my internship at Melexis Technologies, I had the opportunity to participate in the development of a *Hardware-In-the-Loop* platform for the software qualification of a Hall effect magnetic position sensor, the MLX90427. In order to validate its ROM-embedded software, the inputs of its digital controller had to be emulated by a model of the analog front-end of the sensor. The test environment was then automated, for an easy regression testing of the software after each update.

1.1 Melexis Technologies

Melexis Technologies is a Belgian fabless semiconductor company founded in 1989. It supplies sensor and driver integrated circuits, such as inductive and magnetic position sensors, pressure sensors, temperature sensors, current sensors and embedded motor drivers [1]. The business activity is mainly focused on the automotive sector but the company is opening to new markets: micromobility, smart appliances, smart buildings, robotics, healthcare [2]. In 2021, Melexis supplied 1.7 billion integrated circuits, which corresponds on average to 18 chips per car produced worldwide. The company ranks third in the automotive sensors market, behind Bosch and Infineon, with $462 million worth of sales in 2018 [1].

Figure 1: Melexis sites worldwide [2]

The headquarters are located in Ieper, Belgium. The company is however implanted on 18 sites worldwide, in Europe, Asia and the USA.

My master thesis took place in Bevaix, Switzerland. The site counts around 70 people, who are involved in the development of Tire Pressure Monitoring Systems (TPMS)[1], magnetic and inductive position sensors and magnetic current sensors. They take part in the analog design, mixed-signal verification, software development, functional safety, product characterization and customer service of the integrated circuits. An innovation pole is also working on the predevelopment of leading-edge products.

My position in the company My first contribution consisted in building a model of the analog front-end of the sensor to emulate the inputs generation of the digital controller under test. The second part of my work was dedicated to the automation of the hardware-in-the-loop environment for an easy regression testing of the software after each update.

1.2 Angular position sensors: state of the art

Angular position sensors are used to track the trajectory of an object following a circular path. The most popular technologies are reviewed below:

Potentiometric position sensor A movable wiper is linked to a mechanical shaft, which is connected to the object whose position is being measured. When the object moves, the wiper evolves on a resistance track, across which a DC voltage is applied. The output voltage of the sensor being measured from the wiper position, this configuration acts as a tension divider bridge: the resistance between the wiper and the end of the track is proportional to the angular position of the shaft. Potentiometric sensors are low-cost but suffer from low accuracy and poor repeatability.

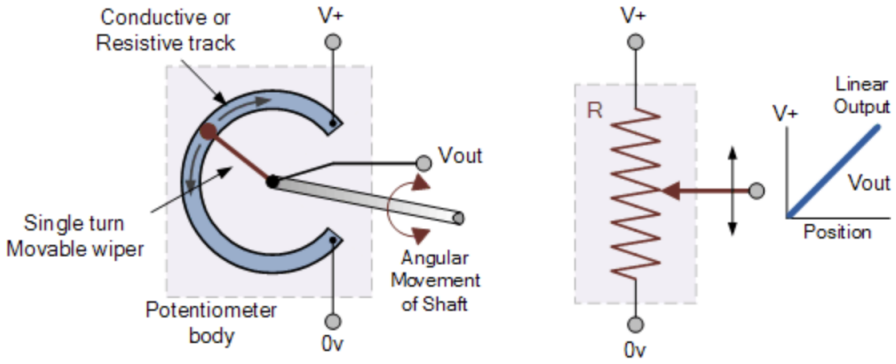

Figure 2: Working principle of a potentiometric position sensor [3]

[1] Low-power microcontroller-based pressure, temperature and voltage sensor

Rotary encoders The angular position of a rotating shaft can be converted into a digital code, using non-contact optical devices, called rotary encoders. Their working principle relies on rotating encoded disks, which are illuminated and scanned by multiple photodetectors to form a stream of binary output pulses. Two types of rotary encoders can be distinguished: incremental rotary encoders and absolute angular position encoders. Incremental rotary encoders make use of simple encoded disks with evenly spaced transparent and dark segments, which are counted to retrieve the relative position of the shaft from its initial position. Two phase-shifted photodetectors are used to determine the direction of the rotation. The resolution of the measurement depends on the number of segments on the encoded disk.

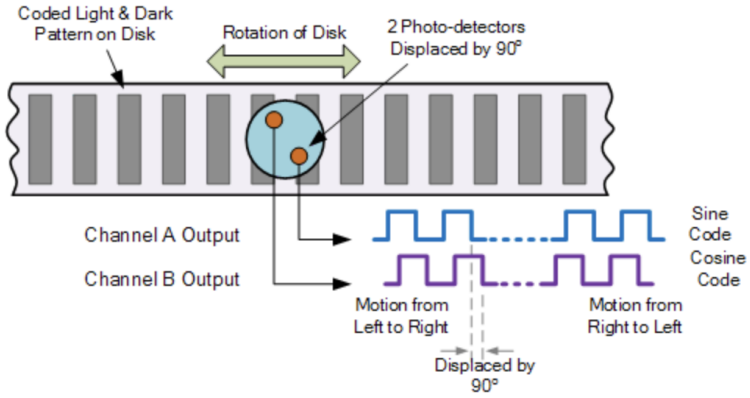

Figure 3: Working principle of a simple incremental decoder [3]

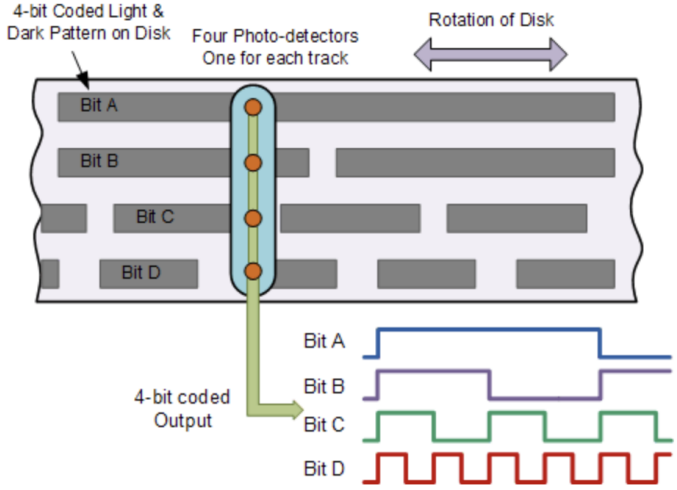

Figure 4: Working principle of a 4-bit absolute position encoder [3]

Absolute position encoders use encoded disks with multiple concentric tracks of light and dark segments, with different spacings, as shown in Figure 4. Each track corresponds to one digit of the encoded output and is scanned by an independent photodetector. The absolute angular position of

the shaft is retrieved by combining the outputs of the different photodetectors. The resolution of the measurement depends on the number of tracks on the disk.

Capacitive position sensors A capacitance can be measured between two conductive plates separated by a dielectric material. The angular position of an object can be retrieved from a capacitance measurement, if the moving object is connected to one of the capacitor plates or to the dielectric material between them [4]. In the first case, the capacitance changes with the displacement because the overlapping area of the plates is altered. In the second case, the dielectric constant of the capacitor varies, as air is introduced between the two plates. Capacitive position sensor are non-contact devices, which allow a high-resolution measurement of the angular position of any conductive target.

Inductive position sensor The electromagnetic induction principle can be used to measure the angular position of an electrically conductive target. Indeed, when an alternating current flows through a detection coil, a changing magnetic field is generated. This magnetic field induces eddy currents in the target nearby [4]. The closer the target, the greater the induced eddy currents are. In return, these eddy currents also generate their own magnetic field, which opposes the magnetic field generated by the coil, changing its impedance [4]. This change of coil impedance can be used to retrieve the angular position of the target. Inductive position sensors offer a contactless, reliable and highly robust position sensing technique. They however only allow the measurement of conducting objects, like metals.

Hall effect-based magnetic position sensors If a flat electrical conductor is crossed by a current and placed in a magnetic field, a voltage can be measured, transverse to the direction of the electrons flow and to the direction of the applied magnetic field. This Hall voltage can be shown to be proportional to the strength of the applied magnetic field. In a Hall effect position sensor, a magnet is connected to the object whose position is to be measured. An object displacement thus alters the strength of the magnetic field being sensed: the Hall voltage becomes an indicator of the position of the object. Hall effect sensors are low-cost and small sensors, which are able to perform accurate, reliable and contact-less position measurements, even in harsh environments. It makes them particularly suitable for the automotive industry, where they are often used for the detection of the pedals positions, the fuel level detection, the turbo charger actuator, etc.

2 Triaxis®

Triaxis® is a patented magnetic sensor technology, which allows precise three-dimensional magnetic field measurement, from a single sensor [1]. It is one of Melexis' most successful products, as the billionth Triaxis® sensor being shipped in 2019. Triaxis® sensors are widely used in automotive position sensing, but also in agricultural vehicles and equipment, joysticks, wheelchairs, and many more [1]. Its working principle relies on the Hall effect and the use of an integrated magnetic concentrator.

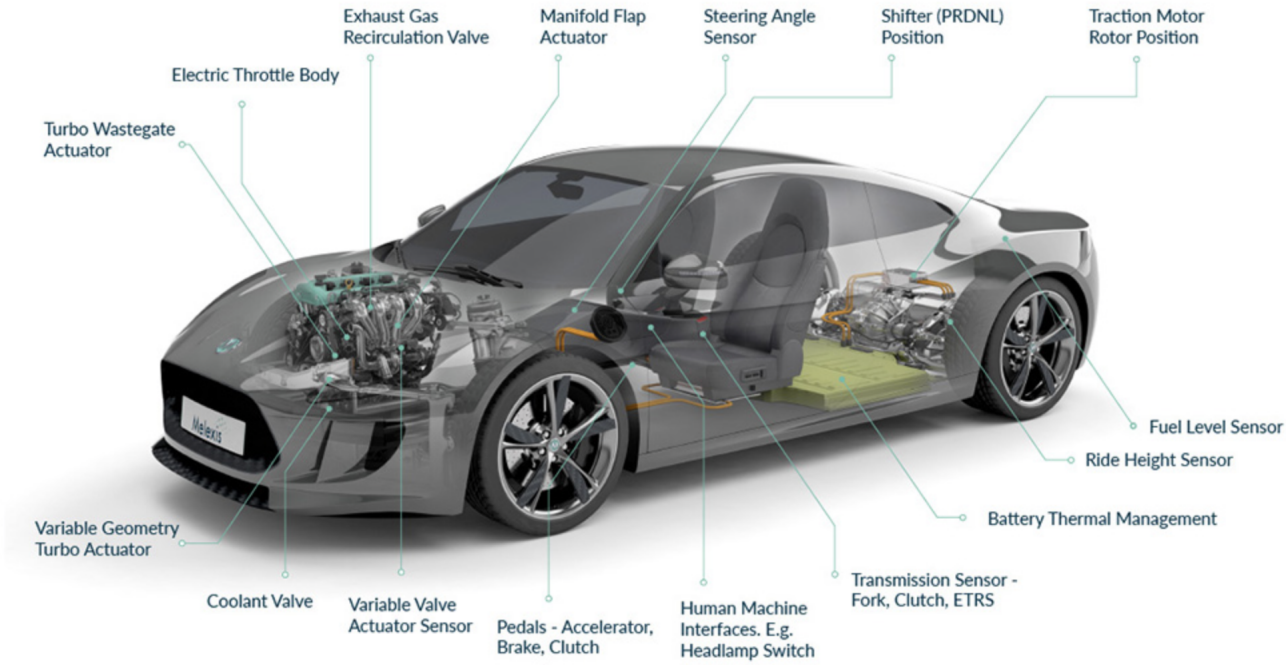

Figure 5: Triaxis® sensors applications in the automotive industry [1]

2.1 Hall effect

The Hall effect was discovered by Edwin Hall in 1879. It manifests itself by a transverse voltage across a conductor, through which an electrical current flows, perpendicularly to an external magnetic field [5].

To better understand its principle, let's imagine a piece of electrical conductor in the xy-plane, on which a voltage V and a vertical magnetic field $\vec{B} = B\vec{u_z}$ are applied. The applied voltage generates an electric field $\vec{E} = E\vec{u_x} = -\nabla V$, which makes the electrons follow a uniform rectilinear, with an average velocity $\vec{v} = -v\vec{u_x}$ [5]. The y-component of the Lorentz force $\vec{F_L} = -e\vec{E} - e\vec{v} \wedge \vec{B}$ starts deviating the electrons in the $-\vec{u_y}$ direction. The accumulation of electrons on one side of the piece of conductor results in an additional electric field, the Hall electric field $\vec{E_H}$ [5]. In the end, the electrons in the conductor undergo both a Lorentz force $\vec{F_L} = -e\vec{E} - e\vec{E_H} - e\vec{v} \wedge \vec{B}$ and a friction force $-\frac{m}{\tau}\vec{v}$. In

steady state, we get:

$$-e\vec{E} - e\vec{E_H} - e\vec{v} \wedge \vec{B} - \frac{m}{\tau}\vec{v} = \vec{0} \tag{1}$$

A projection along the y-axis gives $E_H = vB$: the magnitude of the applied magnetic field can be extracted from the Hall voltage V_H, defined as $\vec{E_H} = -\nabla V_H$ [5]. This is the principle behind the *Hall plates* used in the Triaxis® sensors.

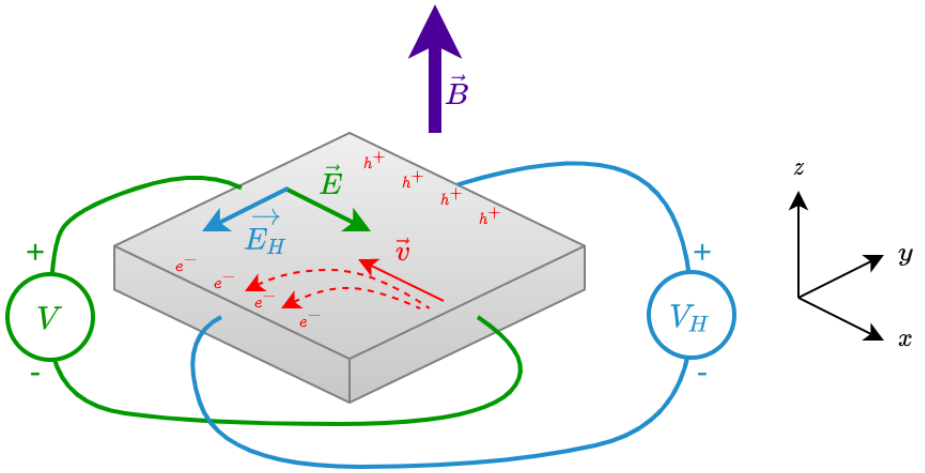

Figure 6: Hall effect in a conductor

2.2 Integrated magnetic concentrator

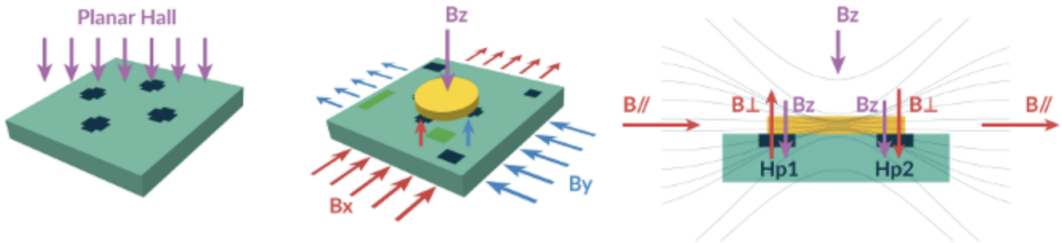

Figure 7: Integrated magnetic concentrator concept [1]

Traditional integrated Hall effect sensors are usually only sensitive to the magnetic field component perpendicular to the surface of the Hall plate. Triaxis® sensors, on the other hand, allow the measurement of the three magnetic field components with a single integrated circuit, through the use of an Integrated Magnetic Concentrator (IMC) [1].

An IMC is a ferromagnetic layer, which can be placed on the surface of a magnetic sensor. It has the ability to locally modify the direction of an external parallel magnetic field: the flux density parallel to the integrated circuit surface is converted into an orthogonal one, suitable for the planar Hall plates.

Hall plates placed near the edge of an IMC can therefore measure both perpendicular and parallel components of an applied magnetic field.

2.3 On-axis rotation angle measurement with a Triaxis® sensor

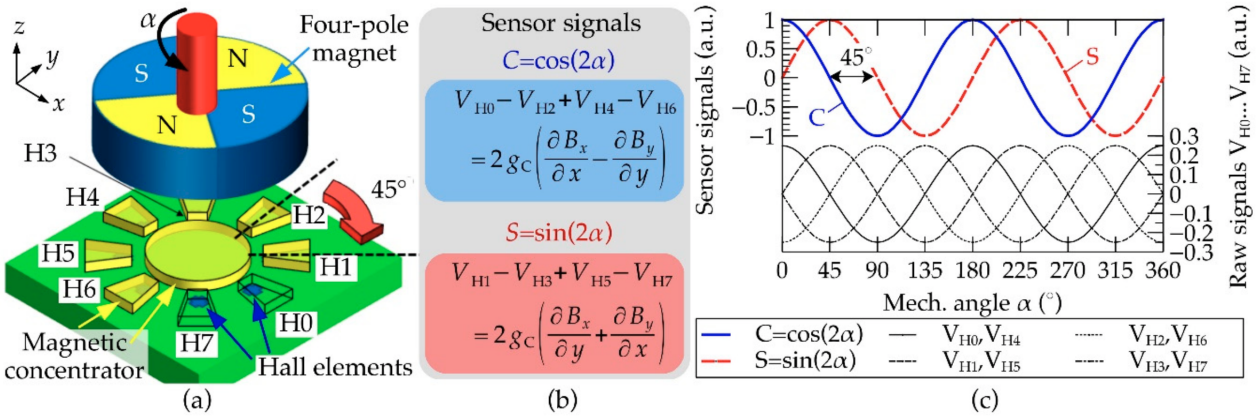

Figure 8: Concept of the rotary position sensor system (a) Four-pole magnet and sensing device consisting of eight circularly arranged Hall elements and a magnetic concentrator. (b) Calculated values of the raw signals and the sensor signals. [6]

To better understand the working principle of a Triaxis® sensor, let's consider the system described in Figure 8: a four-pole magnet rotates on top of an integrated circuit including eight Hall plates and an IMC. The four-pole magnet generates the in-plane magnetic flux gradients $\partial B_x/\partial x$, $\partial B_y/\partial y$, $\partial B_x/\partial y$ and $\partial B_y/\partial x$ [6]. It can be shown that [6]:

$$C = cos(2\alpha) = V_{H0} - V_{H2} + V_{H4} - V_{H6} = 2\, g_C \left(\frac{\partial B_x}{\partial x} - \frac{\partial B_y}{\partial y} \right) \tag{2}$$

$$S = sin(2\alpha) = V_{H1} - V_{H3} + V_{H5} - V_{H7} = 2\, g_C \left(\frac{\partial B_x}{\partial y} + \frac{\partial B_y}{\partial x} \right) \tag{3}$$

α	Angular position of the magnet
K_T	Temperature sensitivity
V_i	Output voltage of the i^{th} Hall plate
g_C	IMC gain

Therefore, the rotation angle can easily be computed from the Hall plates voltages as:

$$\alpha = \frac{1}{2}\, arctan\left(\frac{C}{S}\right) \tag{4}$$

Moreover, unlike conventional magnetic sensors, some Triaxis® sensors can use the in-plane magnetic flux density gradients to become robust to stray magnetic fields [6].

Many types of magnet motions can be easily detected and quantified, besides an on-axis rotation. Different types of magnets and Hall plates configurations can also be used, depending on the wanted resolution and detectable motions: *linear*, *rotary* and *joystick*.

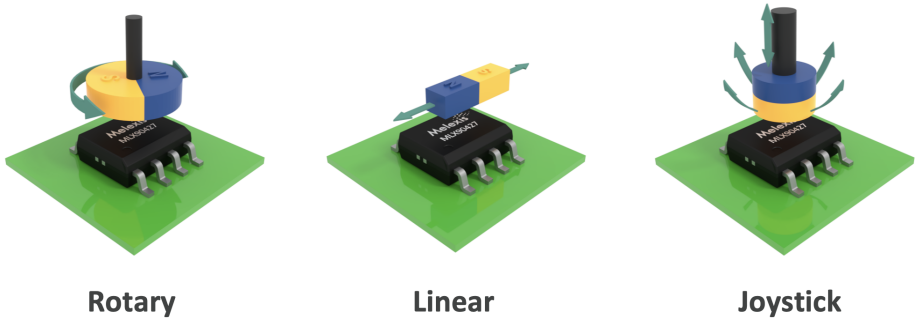

Figure 9: Motions detectable with Triaxis® sensors [1]

2.4 MLX90427

The MLX90427 is a sensor from the Triaxis® product line, with a Serial Peripheral Interface (SPI) for on-demand activity. Its main targeted application is a steering angle sensor, for the measurement of an automotive vehicle steering column angular position. A steering wheel can generally make up to two full turns in each direction, while the typical measurement range of angular position sensors is only one full turn. A common strategy consists in combining the outputs of two position sensors, according to the Nonius/Vernier principle [7]. As the steering angle is used by the Electronic Stability Program (ESP), for the stability control mechanisms of the vehicle, the steering angle sensor should satisfy high safety integrity requirements. It will in fact be classified as an ASIL-D device, which is the highest classification level defined within the ISO 26262 standard (see Section 5.1) and required when a malfunction of the device could be severely life-threatening or cause fatal injuries. Through redundancy, the MLX90427 sensors inside will only be classified as ASIL-B products.

2.4.1 System architecture

The system architecture of the MLX90427 is described in Figure 10. A magnet and an IMC define the magnetic context for sixteen Hall plates. Since the output of the Hall plates is temperature-dependent, a temperature sensor is implemented for compensation. A second temperature sensor is used for diagnostic purposes. The Analog Front-End (AFE) of the integrated circuit includes an amplification chain and an anti-aliasing 1^{st} order filter. A 15-bit Analog-to-Digital Converter (ADC) links the analog part of the circuit to an Amalthea digital platform, which is a highly configurable microcontroller. This microcontroller includes a MLX16 Central Processing Unit (CPU), an ADC controller, an SPI con-

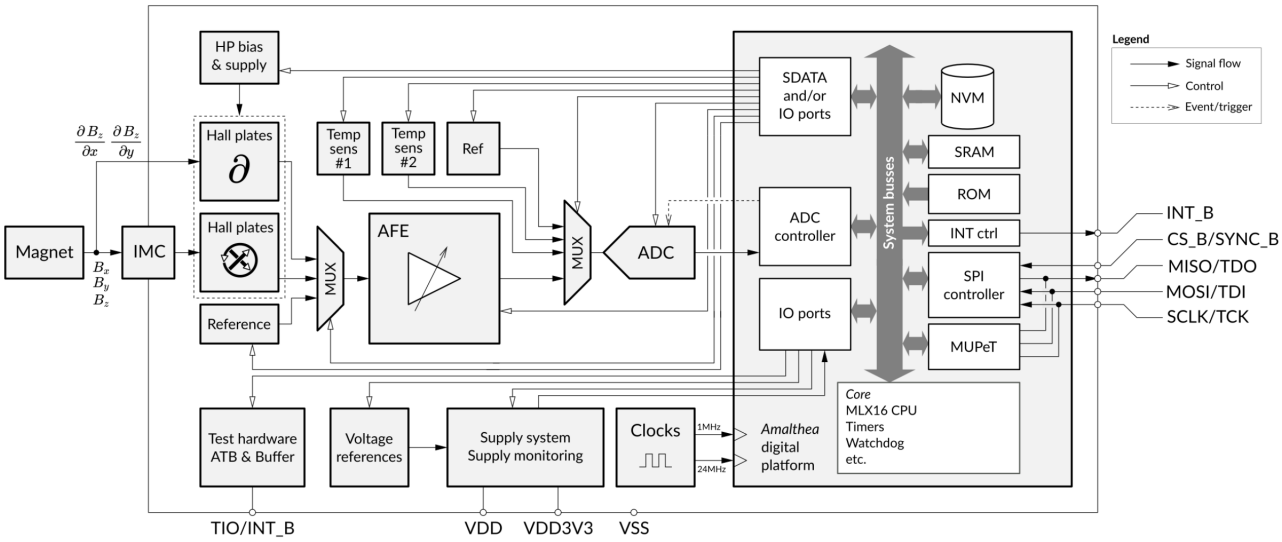

Figure 10: Block diagram of the MLX90427
[Image taken from the MLX90427 specifications]

troller, a Melexis Universal Program and Test (MUPET), an interrupt controller, timers, a watchdog[2], etc. It also includes memories like a Read-Only Memory (ROM) on which the embedded software is stored, a Non-Volatile Random-Access Memory (NVRAM) with parameters to configure the computations performed by the digital controller, and a Static Random-Access Memory (SRAM) to store the temporary variables required during the software execution.

2.4.2 Hall plates configuration

The Hall plates configuration of the MLX90427 is given in Figure 11. There are 16 individual Hall plates, divided into 8 groups (*HP0* to *HP7*). Each group is made of two equivalent Hall plates, for noise reduction. The inner plates, next to the IMC (*HP0* to *HP3*) are the *Legacy plates*. They measure the angular position of a magnet in the xy-, xz- and yz-planes, using the IMC layer. The outer ones (*HP4* to *HP7*) are the *dBz plates*. They measure the angular position of the magnet in the xy-plane, through the computation of the difference between the z-components of the magnetic field, at two opposed sensing points. Such a measurement is therefore insensitive, in first approximation, to stray magnetic field in any direction.

2.4.3 Magnetic modes

Different *magnetic modes* are defined, depending on the type of motion being detected and the Hall plates selected for the magnetic measurements. Depending on the magnetic mode, two, three or

[2]software timer that is used to detect and recover from digital controller malfunctions, by resetting the chip if the internal timer expires without being refreshed

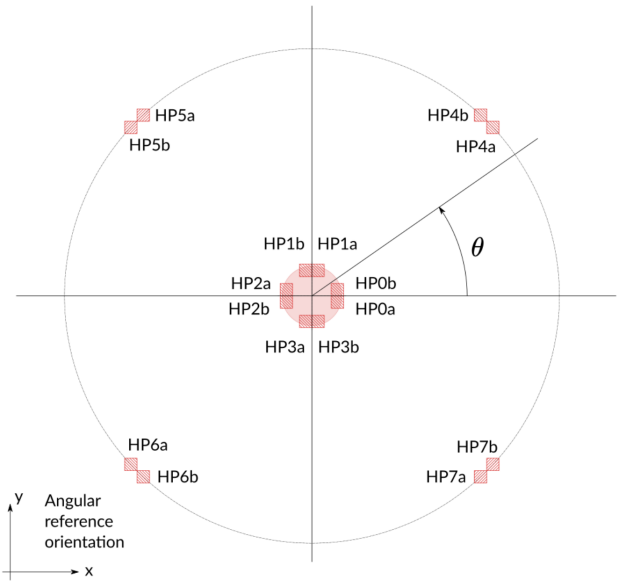

Figure 11: Hall plates system overview
[Image taken from the MLX90427 specifications]

four magnetic field components are measured during an ADATA acquisition sequence.

Mode	Measurement	Plates group	Number of field components
Rotary XY	Angular position projected in the XY-plane	Legacy	2
Rotary XZ	Angular position projected in the XZ-plane	Legacy	2
Rotary YZ	Angular position projected in the YZ-plane	Legacy	2
Rotary dBz	Angular position projected in the XY-plane	dBz	2
Rotary Dual	Angular position projected in the XY-plane	Legacy, dBz	4
Diagnostic Rotary	Angular position projected in the XY-plane	Legacy	4
Joystick XYZ		Legacy	3

When in *Rotary Dual* mode, the angular position of the magnet in the xy-plane is measured with both the *Legacy* and the *dBz* plates. The comparison between the two results allows the detection of a random fault in the system or an error induced by the presence of a stray field. When in *Diagnostic Rotary* mode, the angular position of the magnet in the xy-plane is measured with the *Legacy* Hall plates, once with the full set configuration, and once with only one of the two plates of each group. This mode is used as a safety mechanism, to verify that both measurements provide the same result, except for the systematic angular shift linked to the geometrical arrangement of the plates, and for the slightly higher noise when using half of the Hall plates.

2.4.4 Diagnostics

Three types of AFE diagnostics are implemented in the MLX90427. These three diagnostics are complete after 21 different measurements. A predefined list gives the order in which these measurements have to be executed.

Test-bridge diagnostic The AFE is regularly tested through a test-bridge acting as a controlled input voltage source. The amplification chain is connected to the test-bridge output instead of the Hall plates. Four A/D conversions of four different test-bridge voltage values are performed. These values are stored and used as pairs, as the output voltages of the Hall plates. The following two values are computed and the results compared to hardcoded limits. A fault is reported if the tolerance is exceeded:

$$A = \frac{t_1 - t_0}{2} \tag{5}$$

$$B = \frac{t_3 - t_2}{2} \tag{6}$$

t_i Result of the i^{th} A/D conversion

Temperature diagnostic The outputs of the two temperature sensors are compared. If the difference is higher than a tolerance specificied in the NVRAM , a fault is reported.

ADC diagnostic The ADC is tested through the consecutive measure and A/D conversion of 16 reference voltages. The results are compared to a reference. If the difference between the result and the reference is larger than a hardcoded tolerance, a fault is reported.

2.4.5 ADATA acquisition sequence

The output of the ADC is referred to as *ADATA*. It corresponds to the 15-bit digital value resulting from a magnetic or a diagnostic measurement. When the proper SPI request is sent to the sensor, a full ADATA acquisition sequence is triggered because multiple magnetic measurements are required to compute the position of a magnet at a given time. Indeed, each magnetic field component requires four different measurement phases (see Figure 12), with four different Hall plates biasing configurations. These ”spinning phases” allow cancelling the Hall plates offsets.

The last two phases of each ADATA acquisition sequence are dedicated to diagnostics measurements. The first one is always a temperature measurement performed by the first temperature sensor, for temperature compensation of the magnetic measurements. The second one is selected from the predefined ordered list of 21 diagnostic measurements needed for the AFE diagnostics (see Section 2.4.4). When a Full Diagnostic Sequence (FDS) is triggered via a specific SPI request, the 21 diagnostics measurements are performed in a single sequence, without any magnetic measurement.

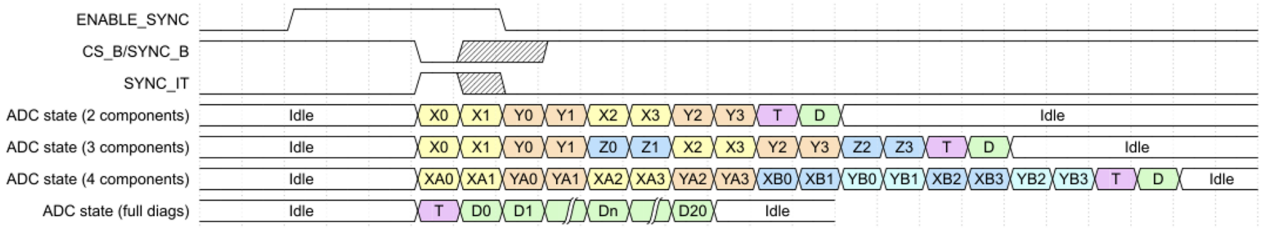

Figure 12: Acquisition sequences
[Image taken from the MLX90427 specifications]

2.4.6 SDATA

Multiple settings are used to configure the analog blocks: Hall plates selection and biasing configuration, test-bridge activation, rough offset and gain selection for the automatic control loop, ADC input selection, etc. These settings are referred to as *SDATA*. At start-up, they are built from ROM look-up tables and parameters stored in the NVRAM, according to the programmed magnetic mode. They are stored in the ROM and accessed through a Direct Memory Access (DMA).

3 Triaxis-Hardware-In-the-Loop

The embedded software of Triaxis® sensors is stored in the ROM of the digital controller. It is verified through mixed-signal simulations and validated in the lab, during the product verification step. Mixed-signal simulations give full visibility of all the signals in the digital controller, for deep debugging. They are however very slow as it takes 2 hours to simulate 500 ms, limiting the test coverage. On the other hand, the product verification involves expensive prototypes, whose packages block the access to the internal signals of the product. Also, discovering a software issue this late in the development process can have a dramatic impact on the development schedule.

Hardware-In-the-Loop simulation would allow to bridge the gap in the testing of the firmware and digital controller of Triaxis® sensors, through the development of a low-cost, real-time and automated integration and validation platform, for early debugging and design optimization.

3.1 Hardware-in-the-loop simulation

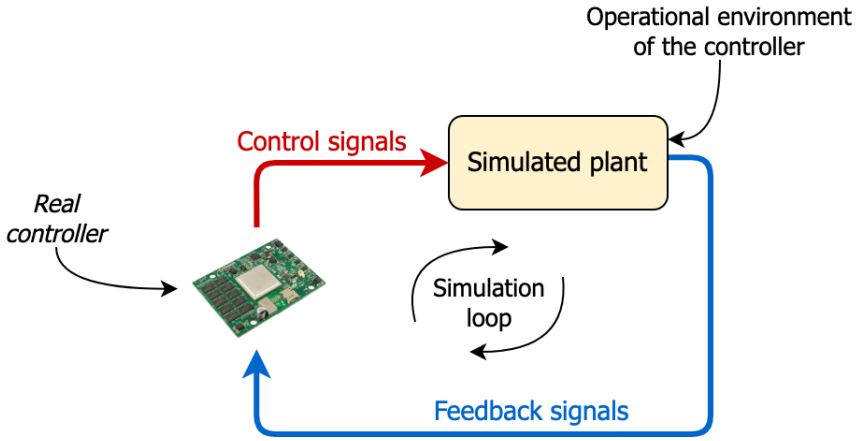

Figure 13: *Hardware-In-the-Loop* concept

Embedded computing is ever more present in safety-critical systems, such as aircraft flight control systems or nuclear reactor controllers. Therefore, reaching a thorough system-level testing[3] coverage, while minimizing the time-to-market, development effort and testing cost, has become an acute need [8].

Hardware-In-the-Loop (HIL) simulation provides comprehensive, repeatable, and low-cost system-level testing [8] by verifying how an embedded system responds in real time to realistic virtual stimuli [9]. The embedded system is removed from its operational environment and interfaced with a plant simulation of the sensors and the actuators it normally interacts with. The plant should be simulated

[3] verifying that the controller, as a whole system, meets both functional and non-functional requirements

on a computer capable of real time performance, along with collection, storage, and analysis of the generated outputs [8].

Significant changes in the hardware or the software should be tested to prevent unintended effects from remaining undetected. With HIL simulation, the embedded system can be tested earlier in the development process. Thus, extensive and economical design optimization and hardware/software debugging can be reached within shorter development schedules [8]. Through the automated generation of control sequences, system-level testing also becomes fast and repeatable. Finally, extreme conditions, such as deep sea, space, fire, or blizzards can be safely and easily reproduced with simple parametric configurations [9].

3.2 Hardware-In-the-Loop simulation for Triaxis® sensors

The Triaxis-Hardware-In-the-Loop (THIL) project consists in splitting the sensor between the AFE and the digital platform. The digital platform becomes the Device Under Test (DUT) and the AFE and the magnetic context become the plant of the HIL simulation.

The AFE is emulated through a MATLAB®/Simulink® model executed on a PC. This PC is interfaced to a Field Programmable Gate Array (FPGA) synthetizing the digital controller and including debugging and controlling options for the validation of the DUT.

Remark. *The THIL projects differs from regular HIL simulation because the DUT is not the actual controller of the sensor, but rather an emulation running on FPGA. However, because the emulated digital controller and the real hardware have the same gate-level design and because the FPGA is cycle-accurate, the emulation behaves as the actual digital controller hardware and can still be considered as such.*

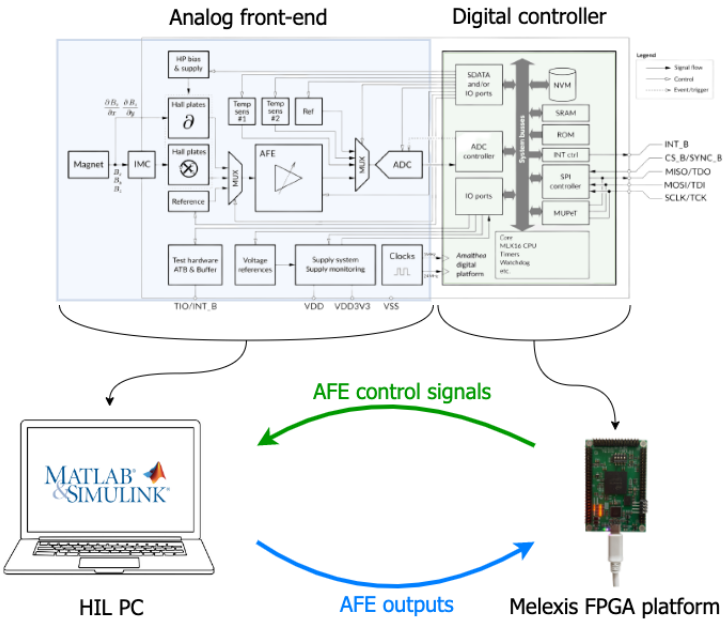

Figure 14: *Triaxis-Hardware-In-the-Loop* concept

3.3 THIL deployed to the MLX90427

HIL simulation is highly recommended for ASIL-B products, like the MLX90427 sensor. Testing the MLX90427 with the THIL platform also allowed to comply with the tight development timeline demanded by the customer.

3.3.1 Realization

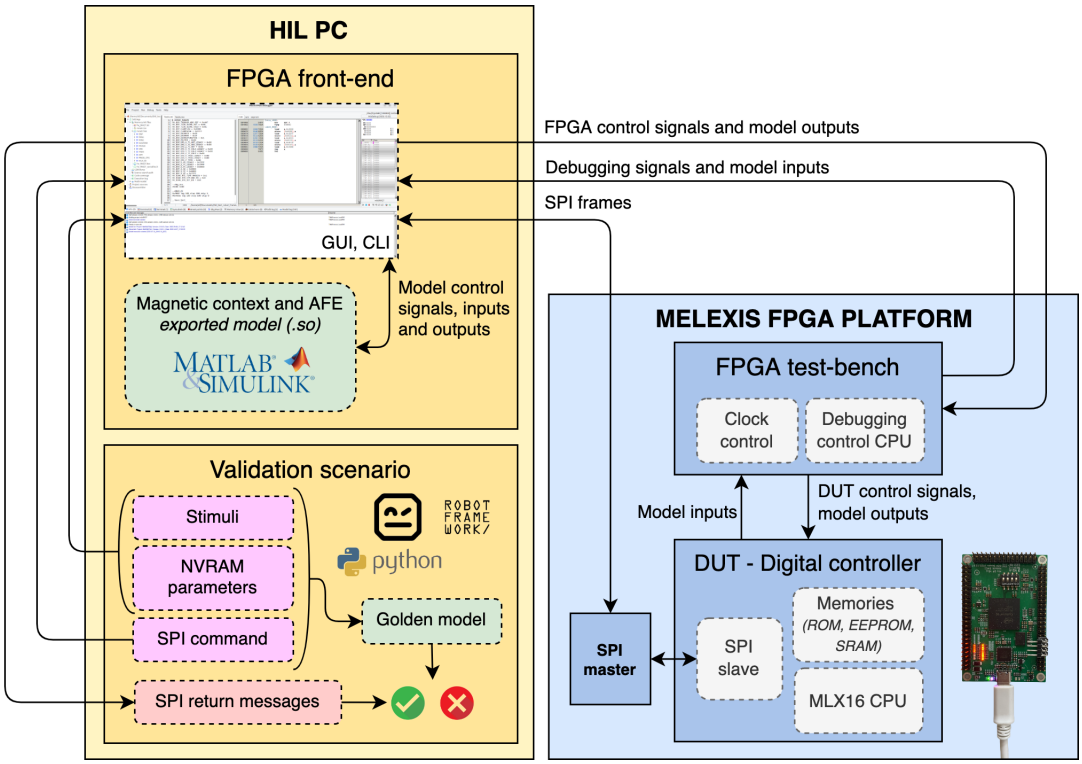

Figure 15: *Hardware-In-the-Loop* concept

The THIL environment of the MLX90427 consists of a Melexis in-house designed FPGA platform, connected to a PC via USB. The FPGA is capable of synthesizing the Amalthea microcontroller, which is the DUT. It also includes a custom-designed test bench with controlling and debugging features of the validation flow, like stopping the Amalthea clock, memory monitoring or code debugging with breakpoints. The environment is commanded from a front-end on the PC. The front-end is also responsible for monitoring the execution of the AFE model, which takes place on the PC itself.

The validation scenario is controlled from a Robot Framework® layer on the PC. Robot Framework® is a generic open-source automation framework, which can be extended with custom Python® modules. Each test case is defined by the stimuli to be applied in the AFE model, some parameters to be stored in the NVRAM, and the SPI commands to be sent. Before each test case, the NVRAM parameters and the stimuli to be applied are transmitted to the FPGA front-end. The SPI commands are sent to the FPGA front-end one by one, through a TCP/IP socket. They are then transmitted to

a SPI master emulated on the FPGA, which is interfaced with an SPI slave inside of the DUT. The corresponding model control signals are generated by the digital platform and sent back to the FPGA front-end, which triggers the AFE model execution. The computed ADATA table is then transferred to the Amalthea platform. The magnet position is computed and the result is communicated by the SPI slave as a SPI return message. This message is received by the SPI master, transmitted to the FPGA front-end and sent back to the Robot Framework® layer though the TCP/IP socket above-mentioned. It is finally decoded and compared to the expected response to validate the software.

3.3.2 Synchronization

A ADATA table computation is triggered by the embedded software when requested through a SPI command received by the digital controller. The AFE model execution takes longer than it would take the actual AFE hardware to perform the required measurements. To give the PC time to complete the model execution before the results are processed by the digital controller, the Amalthea clock is stopped.

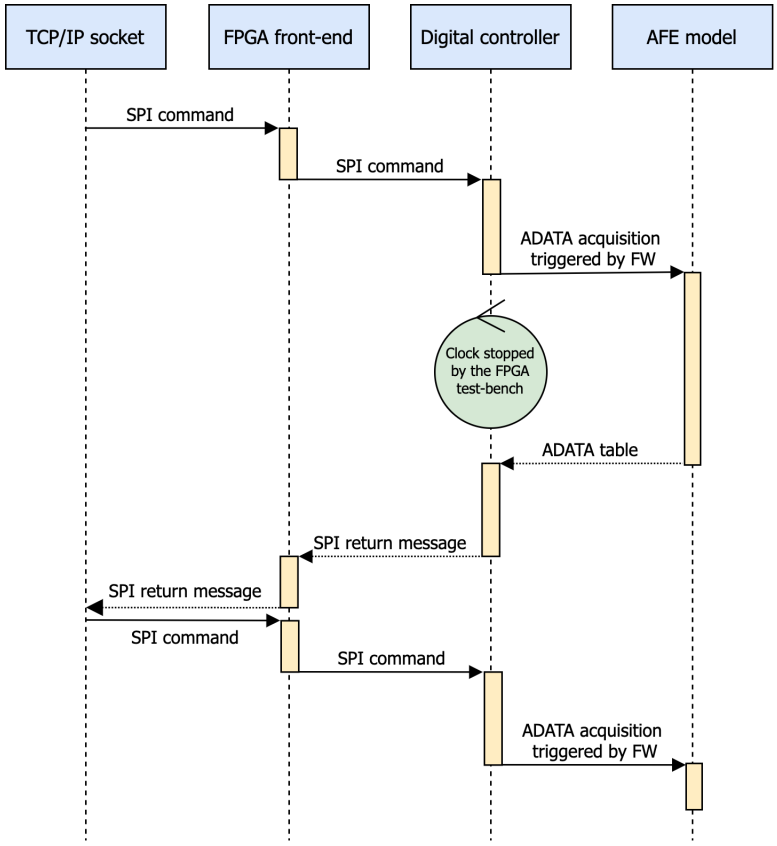

Figure 16: Sequence diagram for the computation of an ADATA table with the THIL

3.3.3 Performance measurement

The delays required by the THIL environment for the processing and transmission of the data were measured in lab. It was shown that the current THIL configuration reaches 43% of real-time performance, which is far beyond the 1/3000 of real-time performance of the mixed-signal simulations currently used for the software verification of Triaxis® sensors. This great result could however be further improved by reducing the time required by the AFE model to compute the ADATA tables. The code generated when compiling the Simulink® model could for instance be optimized.

4 Analog Front-End model of the MLX90427

A timed and behavioral model was developed to simulate the ADATA table acquisition triggered by the digital controller and performed by the AFE of the MLX90427. It is timed because the different measurement phases are scheduled as in the actual sensor. It is also behavioral because it copies the working principle of the AFE of the sensor, without accurately assessing all the system specifications, as the primary goal remains the verification of the embedded software. Therefore, a simplified model was enough for the computation of a meaningful ADATA table.

4.1 Model properties

The *AFE model* of the MLX90427 is in fact a model of the entire analog circuit of the sensor, not only the amplification chain. Indeed, it also emulates the temperature sensors, the Hall plates, the ADC and the selection and execution of the AFE diagnostics. Besides, the magnet and the IMC are also included in the Simulink® model, through the computation of the magnetic field components to be measured by the simulated sensor. On the other hand, the voltage supply system is not modeled, as it doesn't have any impact on the behavior of the AFE, because the digital values computed by the ADC are rescaled according to the supply voltage value. The "spinning phases" (see Section 2.4.5) are also neglected because our ideal Hall plate model excludes any parasitic offset. Also, the anti-aliasing filter can be removed because no signal aliasing occurs in the frequency domain used in the model. Finally, only the automatic regulation of the gain to be applied during the amplification step is modeled. The rough offset correction is a missing feature, which is to be implemented.

Remark. *A Simulink® AFE model had already been done for a previous Triaxis® sensor: the temperature sensor, Hall plate and ADC models were kept identical. The magnetic stimuli generation, the system architecture and the amplification chain were partially reworked to match the specifications of the new MLX90427. Finally, the scheduling of the measurement phases, the SDATA selection, the Hall plates configuration and selection, the shift register and the diagnostics ADATA multiplexer were completely remodeled.*

4.2 Model ports

Model inputs Before each ADATA acquisition sequence, the model inputs are set by the embedded software. For simplicity, they are directly retrieved from the Random-Access Memory (RAM).

Index	Name	Description
1	ADC reset	Indicates when to begin a new ADATA acquisition
2	Measurement mode	Indicates wether a FDS was triggered or not
3	Magnetic mode	Magnetic mode selection (see Section 2.4.3)
4	Virtual gain	Regulated gain computed through a feedback loop
5	Diagnostic counter	Counter to keep track of the current position in the predefined ordered diagnostics list

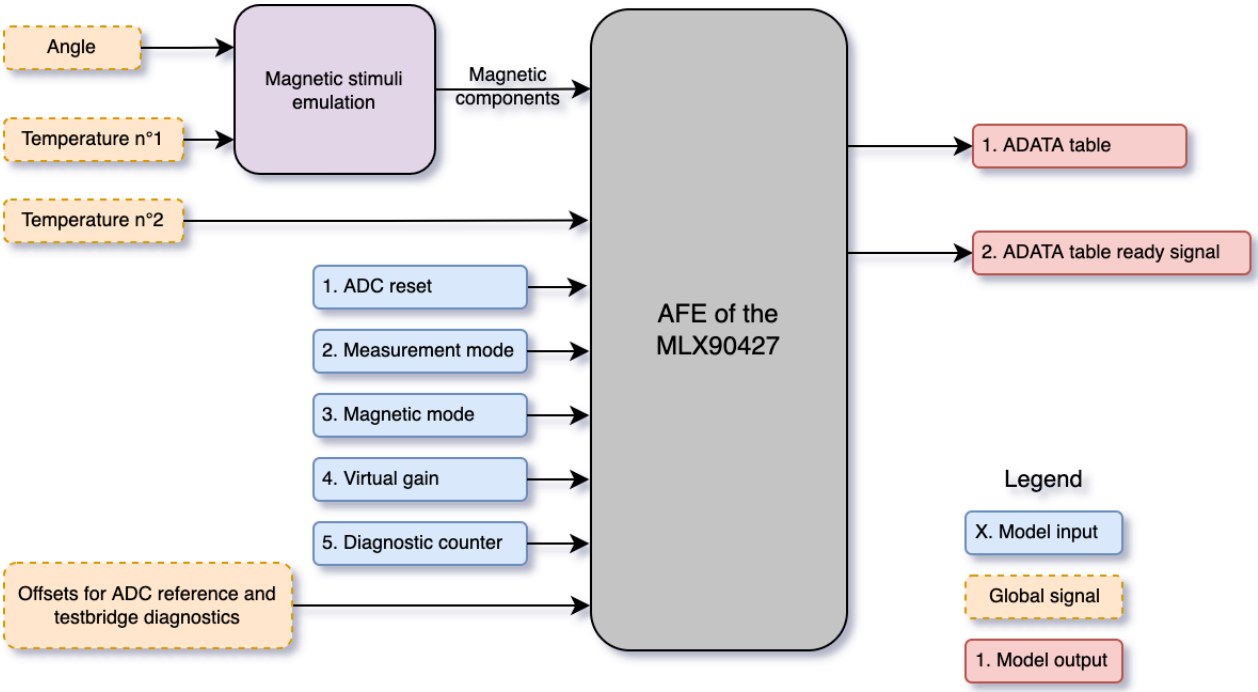

Figure 17: Overview of the Simulink® model

Stimuli Simulink® *global signals* are used to define the stimuli, which can change during the acquisition of a ADATA acquisition sequence.

Name	Description
Angle	Angular position of the magnet
Temperature n°1	Temperature measured by the first temperature sensor
Temperature n°2	Temperature measured by the second temperature sensor
Offset for ADC reference and testbridge diagnostics	15-bit digital value to be added to the default values of the diagnostics results (see Section 4.4)

Model outputs The model outputs are given as inputs to the Amalthea digital platform, on which the software is run.

Index	Name	Description
1	ADATA table ready	Indicates when the ADATA table computation is over
2	ADATA table	Array containing the magnetic and diagnostics components computed during the ADC acquisition sequence

4.3 Magnetic stimuli emulation

Stimuli reference tables were provided by the analog designers of the MLX90427. These tables provide a model of the magnetic component measured by each Hall plate, as a function of the angular position of the magnet. These data were fitted using a simple sinusoidal model and included in the Simulink® model.

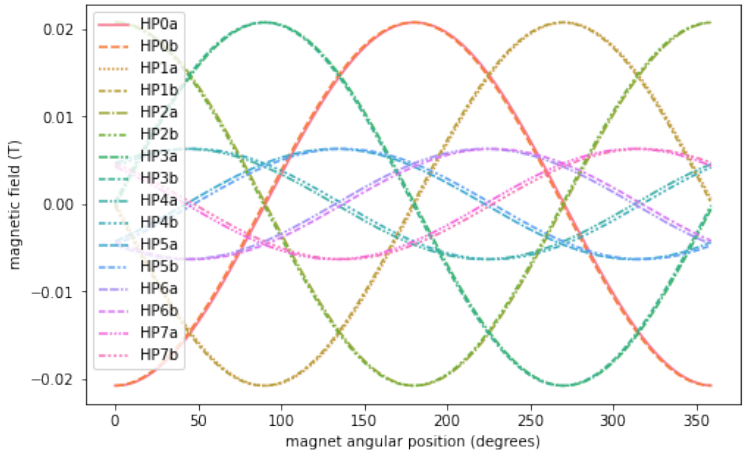

Figure 18: Magnetic components measured by the Hall plates

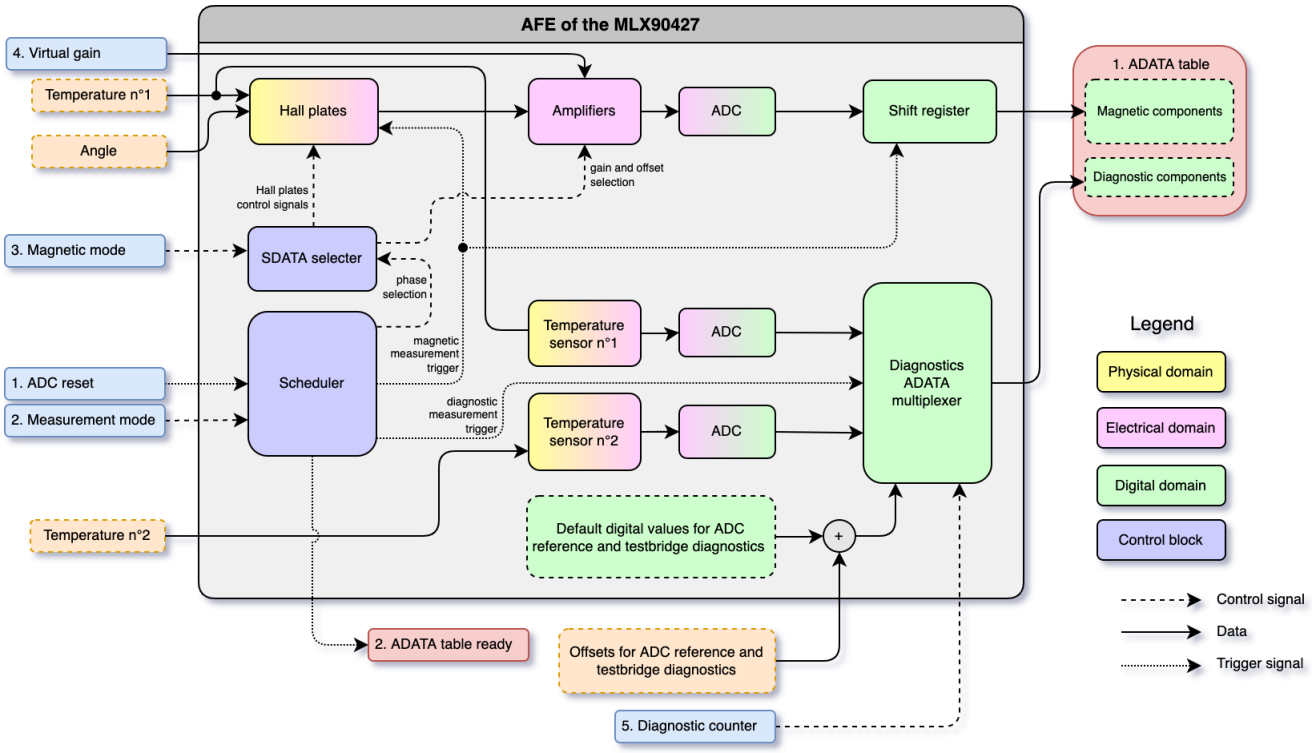

Figure 19: Analog front-end model of the MLX90427

4.4 Model blocks

Figure 19 provides a detailed description of the model blocks. The values of the parameters used in the model are given in the Annexe A.1.

Scheduler When the *ADC reset* input triggers the beginning of a new ADATA acquisition sequence, the scheduler block starts triggering the different magnetic and diagnostic measurement phases. When a *FDS* is triggered through the *Measurement mode* input, 21 diagnostics measurements are run in the same sequence, without any magnetic measurement. The scheduler also indicates when the computation of the entire ADATA table is over, through the *ADATA table ready* output.

SDATA selecter Before each measurement phase, the control signals for the analog blocks are extracted from the SDATA table, depending on the programmed magnetic mode. These signals include the enable signals for the Hall plates and the selection of the gain to be applied in the automatic control loop. The SDATA table is loaded inside the AFE model. In the real sensor, it is stored in the ROM and accessed through DMA.

Temperature sensors The temperature sensors convert a temperature defined by the stimuli into a voltage V_T. To make the two sensors have opposite polarities, as required by the system specifications, the output voltage of the second temperature sensor is flipped. The same linear model is used for both sensors:

$$V_T = K_T \times (T - T_{nominal}) + S \times K_S \times V_{DD} \tag{7}$$

V_T	Output voltage of the temperature sensor
K_T	Temperature sensitivity
T	Temperature
$T_{nominal}$	Nominal temperature
S	Stress
K_S	Stress sensitivity
V_{DD}	Supply voltage

Remark. *The simple linear model of the temperature sensors is unrealistic. However, the temperature computation performed by the software can be trimmed with NVRAM parameters, to make it match the model behavior.*

Hall plates The Hall plates configuration of the MLX90427 presented in Figure 11 is reproduced inside of the AFE model. Each Hall plate measures one of the 16 magnetic field components generated by the *Magnetic stimuli emulation* block. The control signals for the Hall plates are provided by the *SDATA selecter* block. For each measurement phase, these control signals define which Hall plates should be enabled and how they should be biased. Two Hall plates groups are always selected at

once and their outputs are both sent to the amplification chain. The Hall plate model developed for the MLX90377 was kept as is for the AFE model of the MLX90427, since the same Hall plates are implemented in both sensors. This model is based on a second order interpolation of characterization data:

$$V_{Hall} = \pm\, B \times V_{bias} \times (1 + S_{mismatch}) \times S_T \tag{8}$$

with

$$S_T = S_{abs} + \left(1 + S_{rel} \times (T - T_{nominal}) + S_{rel^2} \times (T - T_{nominal})^2\right) \tag{9}$$

V_{Hall}	Output voltage of the Hall plate
B	Magnetic field component read by the Hall plate
V_{bias}	Bias voltage of the Hall plate
$S_{mismatch}$	Sensitivity mismatch
S_T	Temperature sensitivity
S_{abs}	First order absolute temperature sensitivity
S_{rel}	First order relative temperature sensitivity
S_{rel^2}	Second order absolute temperature sensitivity
T	Temperature
$T_{nominal}$	Nominal temperature

Amplifiers The gain to be applied in the automatic control loop of the analog chain is selected according to the SDATA. The output voltages of the two Hall plates groups selected for the measurement are added together and amplified according to the following idealistic model:

$$V_{amp} = 8 \times 1.07^A \times V \tag{10}$$

V_{amp}	Output voltage of the amplification chain
A	Gain selected for the automatic control of the analog chain
V	Sum of the output voltages of the two selected Hall plates groups

Analog-to-Digital converter The ADC model converts the difference between its two inputs voltages, V_P and V_N, into a 15-bit digital value.

$$q = \begin{cases} 0 & \text{if } V < -V_{DD}/2 \\ 2^{15} - 1 & \text{if } V > V_{DD}/2 \\ 2^{14} - 1 + V/V_{DD} \times 2^{15} & \text{otherwise} \end{cases} \tag{11}$$

q	Result of the A/D conversion
$V = V_P - V_N$	Difference of the inputs
V_{DD}	Supply voltage

Shift register This block acts as a shift register. It stores the magnetic measurement results coming serially from the ADC into a table.

Diagnostics ADATA multiplexer When a diagnostic measurement is triggered by the *Scheduler*, the *Diagnostics ADATA multiplexer* block selects the right diagnostic to be executed. For the first diagnostic measurement phase of each ADATA acquisition sequence, it takes the output of the first temperature sensor. For the second diagnostic measurement phase, it chooses amongst the predefined ordered list, according to the *Diagnostic counter* value. If a temperature measurement has been selected, it takes the output of the second temperature sensor. Otherwise, when the ADC reference or a testbridge diagnostic has to be run, a default value is added to an offset. These default values correspond to the 15-bit value ideally expected by the software. The offsets are defined as part of the stimuli and are used to make the result of a diagnostic exceed the tolerance and trigger a fault.

4.5 Results

The functionality of each block of the model was validated with unit tests. The AFE model was then compiled, exported as a *shared object* file and tested as a whole. As an example, the results of the ADATA table computation with the following inputs are presented in Figure 20, where *ADATA i* is the result of the i^{th} measurement:

Angle	$0 \longrightarrow 360°$
Temperature n°1	$0 \longrightarrow 100°C$
Temperature n°2	$0 \longrightarrow 100°C$
Diagnostics offsets	0
Magnetic mode	Rotary XY
Measurement mode	Not an FDS
Virtual gain	20

As expected, the 15-bit digital values are centered around the mid-range value, which is $2^{14} - 1 = 16383$. The sinusoidal trend of the curves is in agreement with the magnetic components being measured by the Hall plates, when the magnet makes a full turn, as shown in Figure 18. Also, as expected from Figure 12, eight magnetic measurements are required to compute the angular position of the magnet when in *Rotary XY* mode, because two magnetic field components are being measured. *ADATA 0* and *ADATA 4* correspond to the measurement of the first magnetic field component and *ADATA 1* and *ADATA 5* to its opposite. *ADATA 2* and *ADATA 6* correspond to the measurement of the second magnetic field component and *ADATA 3* and *ADATA 7* to its opposite. The amplitude reduction with time is explained by the temperature sensitivity of the Hall plates, as modeled by the Equation 10.

The last two measurements are diagnostic measurements. *ADATA 8* corresponds to the temperature measurement performed by the second temperature sensor and its linear trend is congruent with the applied stimuli. *ADATA 9* is the result of the ADC reference and testbridge diagnostics. It was checked that the values presented in Figure 20b match the default values specified inside of the Simulink® model, because no additional diagnostics offsets were applied.

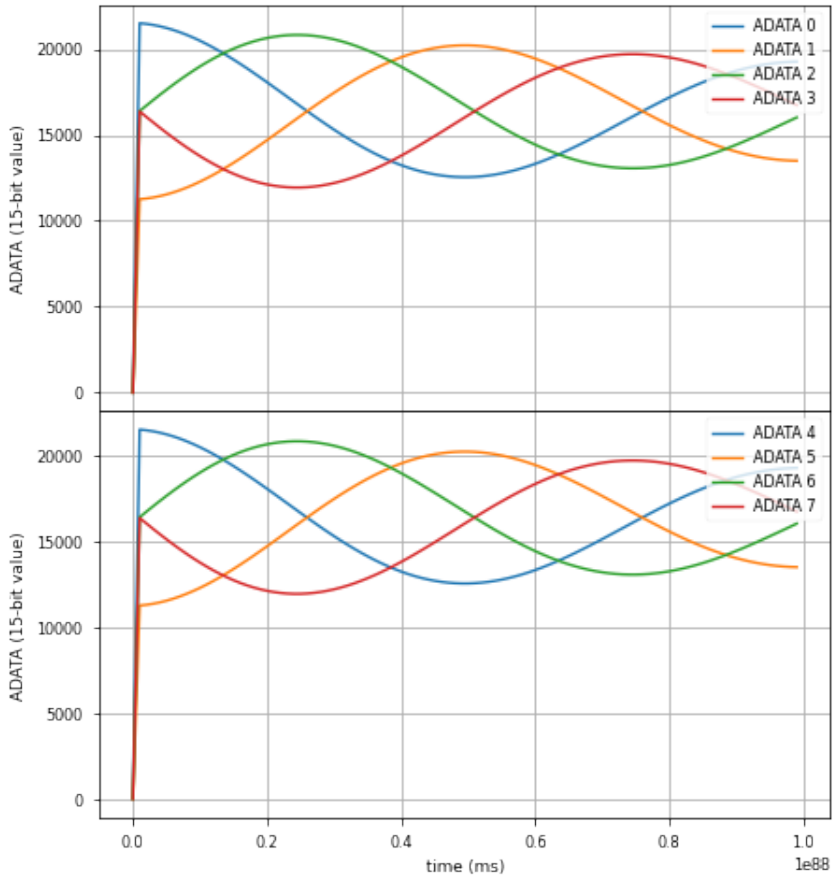

(a) Magnetic measurements results

$$ADATA\,0 = ADATA\,4 = +B_x,\ ADATA\,1 = ADATA\,5 = -B_x,$$
$$ADATA\,2 = ADATA\,6 = +B_y,\ ADATA\,3 = ADATA\,7 = -B_y$$

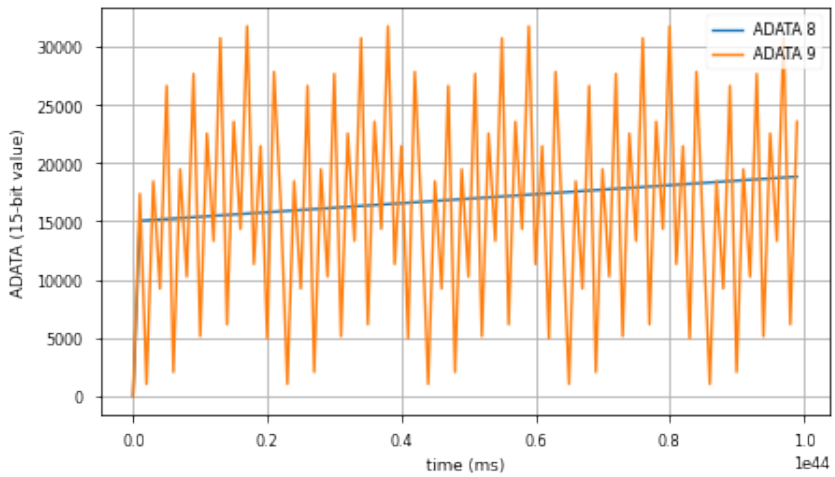

(b) Diagnostics measurement results

Figure 20: ADATA table computed in the *Rotary XY* mode

5 Software qualification tests of the MLX90427

The software qualification of the MLX90427 is performed within the context of the ISO 26262 and the Automotive SPICE® standard. While the ISO 26262 covers the functional safety aspects of the embedded software, the Automotive SPICE® evaluates the quality of its development process.

5.1 ISO 26262

With the increasing complexity of electrical, electronic and software components in automotive vehicles, addressing the risk of random hardware failures and systematic failures has become critical. The ISO 26262 is an international functional safety standard, which aims at mitigating these risks by providing guidance, through the definition of appropriate requirements and processes [10]. Functional safety features now form an integral part of the products development process, production, process management, product operation and disassembly.

5.1.1 Automotive Safety Integrity Levels

The ISO 26262 provides a risk-based approach, through the definition of integrity levels, the Automotive Safety Integrity Level (ASIL) [10]. This qualitative assessment of potential hazards allows to better determine the safety requirements, which are necessary to ensure that an acceptable safety level is achieved. Four different levels are defined: ASIL-A, ASIL-B, ASIL-C and ASIL-D. ASIL-D refers to the most stringent level of safety measures, which is to be applied when a system malfunction could be life-threatening or cause fatal injury (airbags, electric power steering, etc.). On the other hand, ASIL-A is applied when the lowest integrity requirements are sufficient, like for accessory features (rear lights, navigation system, etc.).

5.1.2 Reference process model

The ISO 26262 is based upon a specific reference process model, which specifies the different phases of product development. It is divided in twelve parts, which are further detailed in Figure 21 [10]:

1. Vocabulary
2. Management of functional safety
3. Concept phase
4. Product development at the system level
5. Product development at the hardware level
6. Product development at the software level
7. Production, operation, service and decommissioning

8. Supporting processes
9. Automotive Safety Integrity Level (ASIL)-oriented and safety-oriented analysis
10. Guidelines on ISO 26262
11. Guidelines on application of ISO 26262 to semiconductors
12. Adaptation of ISO 26262 for motorcycles

Only the *Product development at the software level* will be tackled within the scope of this report.

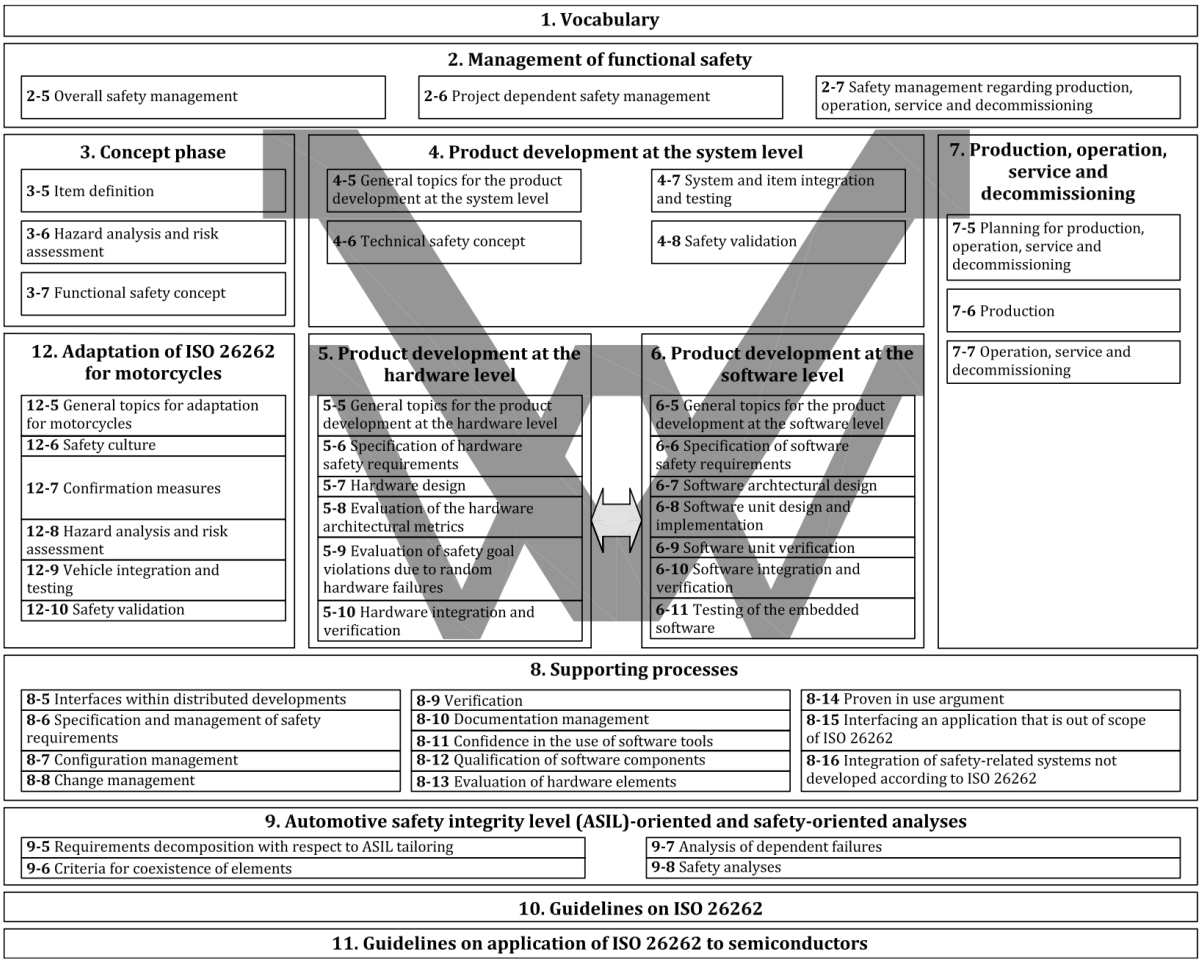

Figure 21: Overview of the ISO 26262 reference process model [10]

5.1.3 Product development at the software level

According to the ISO 26262, the software development should be divided in 6 steps [10]:

- **Specification of software safety requirements:** derive the software safety requirements, corresponding to the correct ASIL, from the technical safety concept and the system architectural design specifications
- **Software architectural design:** develop a software architectural design, which is compliant with the software safety requirements
- **Software unit design and implementation:** develop a software unit design compliant with the software architectural design, and implement the corresponding software units
- **Software unit verification:** provide evidence that the implemented software units are compliant with the expected design and satisfy the software requirements
- **Software integration and verification:** assemble the software elements to form the integrated software and verify that the safety requirements are satisfied at the architectural level
- **Testing of the embedded software:** provide evidence that the software, as a whole, fulfills the software safety requirements when executed in the target environment.

HIL is recommended as a test environment for conducting the software testing process. A software verification report should be provided to evidence the compliance of the software with its safety-related requirements.

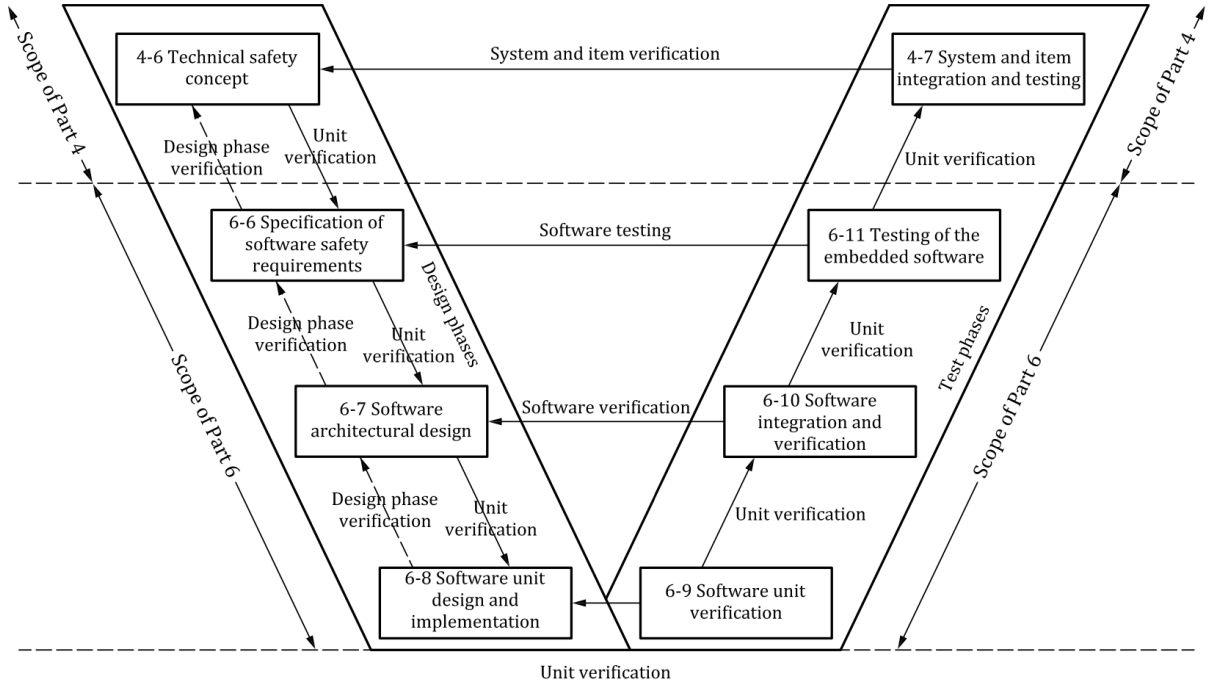

Figure 22: Reference phase model for the product development at the software level [10]

5.2 Automotive SPICE®

Automotive SPICE® stands for Automotive Software Process Improvement and Capability Determination. It was introduced in 2001 by the Automotive Special Interest Group, which includes automotive equipment manufacturers, the Procurement Forum and the SPICE User Group [11]. This widely recognized process assessment model aims at assessing the quality of the development process of Electronic Control Unit (ECU) suppliers for the automotive industry. It involves defining effective guidelines for the development of high quality embedded software.

5.2.1 Process reference model

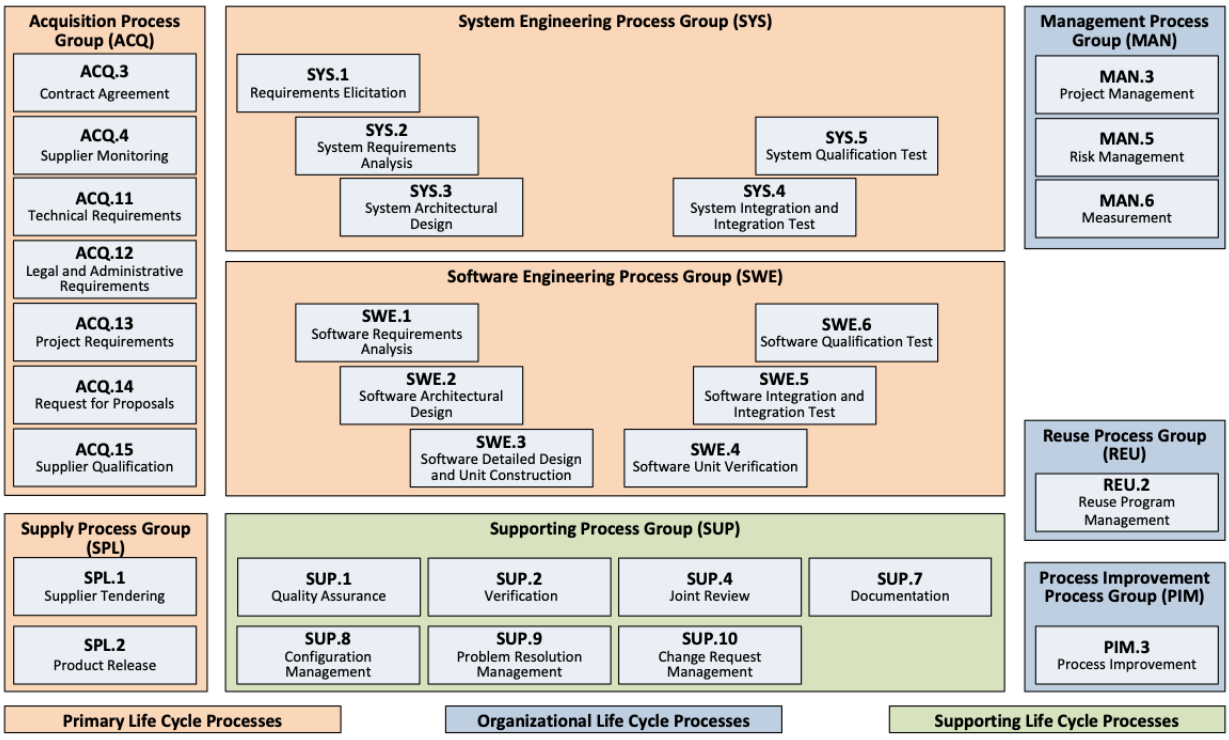

Figure 23: Overview of the Automotive SPICE® process reference model [11]

The Automotive SPICE® defines three process categories. Each category is divided into multiple process groups [11].

- **Primary life cycle processes:** customer acquiring a product from the supplier, supplier engineering and delivering a product to the customer
  - Acquisition Process Group (ACQ)
  - Supply Process Group (SPL)
  - System Engineering Process Group (SYS)

  - Software Engineering Process Group (SWE)

- **Organizational life cycle processes:** help the organization achieve its business goals, through process improvement, and project and resource management
  - Management Process Group (MAN)
  - Reuse Process Group (REU)
  - Process Improvement Process Group (PIM)
- **Supporting life cycle processes:** processes to be employed during the life cycle of the product
  - Supporting Process Group (SUP)

In what follows, only the Software Engineering process group (SWE) will be discussed.

5.2.2 Software Engineering process group (SWE)

The Software Engineering Process Group (SWE) includes management of software requirements, development of the software architecture and design, along with implementation, integration and testing. This process group is partitioned into six different processes [11]:

- **Software Requirements Analysis (SWE.1):** setting the software requirements from the system requirements
- **Software Architectural Design (SWE.2):** defining a software architecture in agreement with the software requirements
- **Software Detailed Design and Unit Construction (SWE.3):** providing a detailed software design with specific software units
- **Software Unit Verification (SWE.4):** verifying that the software units are compliant with the software detailed design and the non-fonctional software requirements
- **Software Integration and Integration Test (SWE.5):** integrating the software units into larger software items and testing their compliance with the software architectural design
- **Software Qualification Test (SWE.6):** making sure the integrated software is compliant with the software requirements

Within the framework of my work, only the SWE.6 process was considered. According to the Automotive SPICE® reference model [11], it should:

- define qualification test specifications with test cases proving the integrated software compliance with the software requirements
- include a regression test strategy to easily re-test the integrated software when it is modified

– allow saving the test results and logs for evidence and communication

– establish bidirectional traceability between the software requirements and the defined test cases

– be executed through hardware debug interfaces or simulation environments (e.g. Software-In-the-Loop simulation or Hardware-In-the-Loop simulation)

5.3 THIL for software qualification

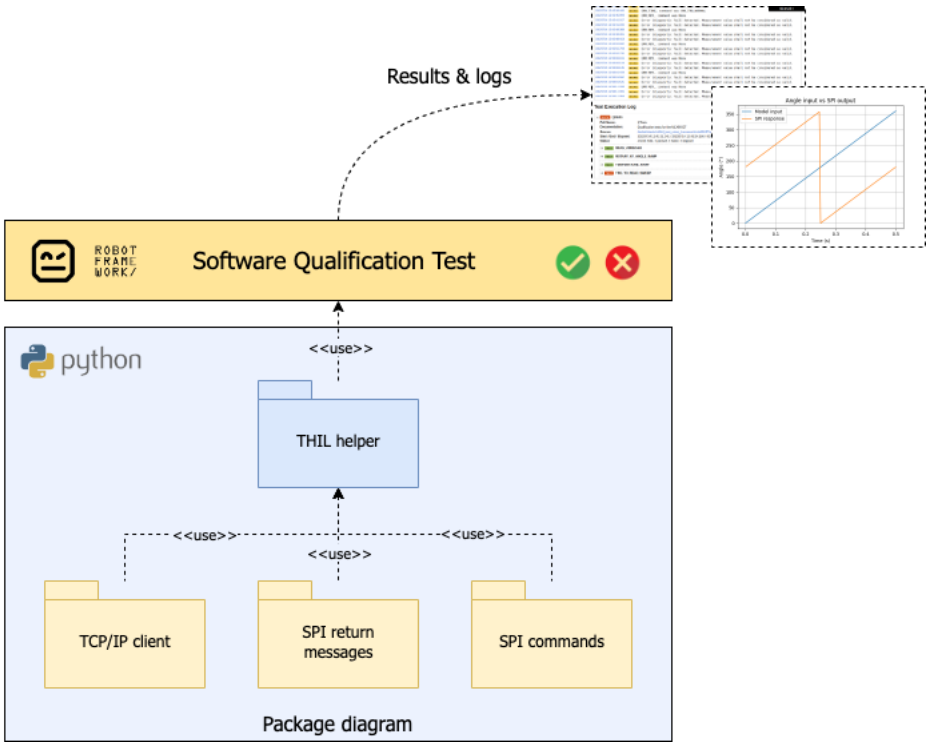

Figure 24: Architecture of the software qualification test environment on the THIL

The ISO 26262 and the Automotive SPICE® provide two process reference models with a different purpose, but a very similar structure. For both models, the last step of the software development process consists in verifying that the software requirements are fulfilled, wether they are safety-related or not. In what follows, this verification step will be referred to as *software qualification*. The ISO 26262 and the Automotive SPICE® both recommend HIL simulation as a test environment. The software qualification of the MLX90427 will thus be executed on the THIL platform, which was described in the Section 3. To this end, a Robot Framework® layer was designed for the definition of the test cases and the control of the THIL platform. Robot Framework® is an open-source automation framework with an easy syntax and human-readable keywords. Its built-in features were supplemented by custom Python® libraries:

– **THIL Helper:** The control of the FPGA front-end is completely automatized:

- The AFE model execution is automatically triggered at the beginning of a test case and terminated at the end.
- The EEPROM parameters and stimuli to be applied are also automatically updated.
- The SPI commands to be sent are easily selected and configurable.
- The SPI return messages are decoded and compared to the expected response. Any error message or measurement error is automatically reported.
- The logs and results of each test case are saved after each execution.

— **TCP/IP client:** The socket used for the TCP/IP communication with the FPGA front-end is connected to the right host and port. The SPI commands are sent and the corresponding SPI return messages are received

— **SPI commands:** The commands to be sent to the MLX90427 are encoded according to the SPI protocol defined in the system specifications

— **SPI return messages:** The return messages received from the MLX90427 are decoded according to the SPI protocol defined in the system specifications. The different fields read from the return messages are provided in a readable format.

5.4 Continuous Integration

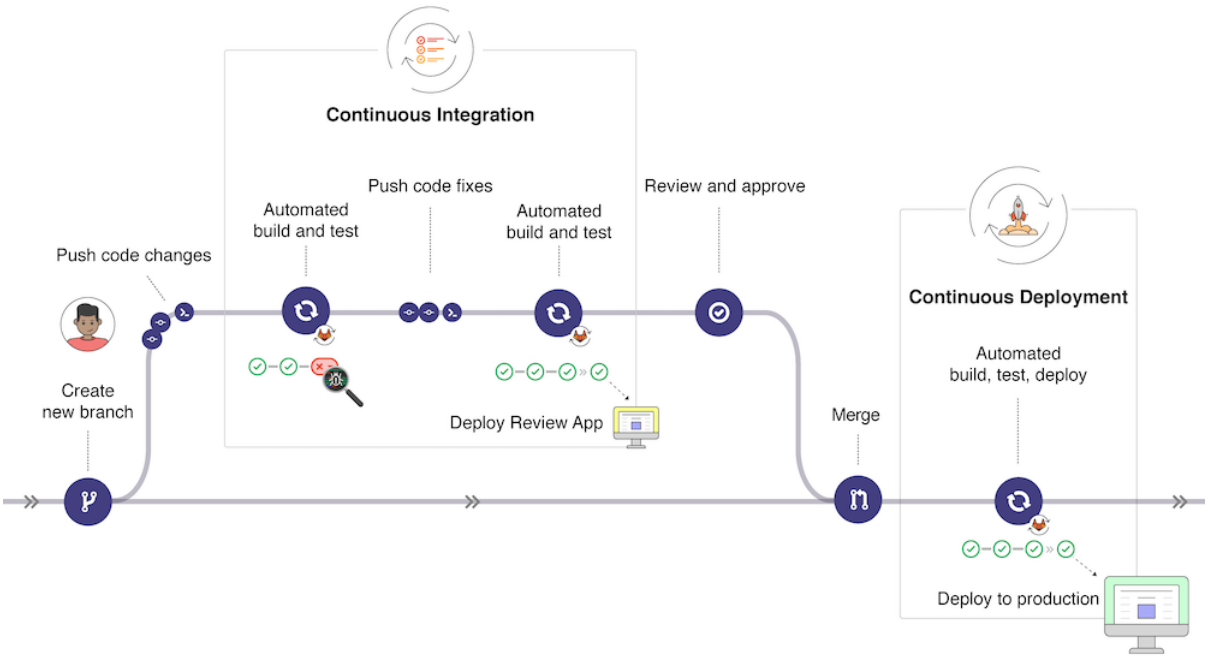

Figure 25: Continuous integration workflow [12]

Continuous Integration (CI) refers to an iterative software development method, which aims at reducing the amount of manual steps required before the deployment of a new piece of code. Let's

imagine multiple developers working on the same project, which is stored in a remote repository. When something has to be fixed, a developer creates a new branch, which is an independent copy of the original code, the *master*. The developer applies the modifications and pushes them to the working branch. After every push, the new code is automatically built and tested to detect any bug introduced by the modifications. Once all the tests are passing, the code is reviewed. If approved, the changes are merged into the master and deployed. This set of practices allows code changes to be applied more frequently and reliably, for a better collaboration and code quality.

As for now, the software qualification tests have been introduced in the CI process of an isolated repository, with files manually copied from the MLX90427 software repository. This step acts as a proof of concept before the integration in the actual CI process of the Software Competency Center (SWCC), for automatic regression testing of the MLX90427 software after each update.

5.5 Outcome

After each release, the software of the MLX90427 was tested with the THIL. Thanks to the near real-time performance of the platform, longer scenarios could be emulated in a very short time, which cannot be done with pure simulation. Thanks to that, multiple bugs were found and corrected very early of the development process.

6 Conclusion

6.1 Project conclusion

The MLX90427 was successfully integrated in a HIL environment. Meaningful SPI return messages were received from the sensor, confirming that both the THIL platform and the AFE model were correctly developed. Thanks to the near real-time performance of the platform and facilitated test execution allowed by the automation of the THIL environment, the embedded software of the MLX90427 was easily tested after each internal release. Multiple bugs were detected and rapidly corrected very early in the development process. After the complete definition of the software requirements, test cases will have to be written for an exhaustive testing of the software. The THIL platform is however still a work in progress, which has to be further corrected and improved. A thorough validation step will also be necessary to guarantee its accuracy. Only then the THIL may be used as an independent and reliable test environment for the products developed by Melexis. Indeed, the project will very likely be deployed to other Triaxis® sensors and other product lines.

6.2 Personal review

I have only good things to say about my internship at Melexis Technologies. Being a part of the THIL project was a great experience. It was very nice to take part in the weekly meetings and to understand the issues at stake when working on such an interesting and multidisciplinary project. Following its evolution over a longer period of time allowed me to get more familiar with the subject and to have more responsibilities. It also allowed me to consolidate the knowledge I have acquired during my studies, while learning many more things, like the working principle of a complex Hall effect sensor or the development process of an embedded software. I also got better at Simulink® and Python®. The thing that surprised me the most during my internship was that a lot of things can be ”learned by doing”. Indeed, many ressources can be found on the internet or in books. Acquiring new competences by yourself is also very rewarding. During my internship at Melexis Technologies, I discovered that I prefer working in the industry, rather than in the research field. Indeed, I prefer taking part in a larger project, which involves a lot of people, with shorter term tasks. I also enjoy the idea of participating in the development of a product, which will actually be commercialized and used by people. Finally, this internship confirmed my taste for software development, which I discovered at the beginning of my studies at Grenoble INP - Phelma. I am very happy to announce that I was offered an Associate Software Engineer position at Melexis Technologies, and that I will get to work again with the amazing people I met during my internship.

6.3 Timeline of the internship

My internship at Melexis Technologies lasted 26 weeks, from 14 February to 12 August 2022. The main tasks, which were accomplished were the following:

— **Triaxis® induction** *(14/02 - 25/02)* After a general introduction of the company activities and

products, I was explained the working principle of Triaxis® sensors, and more specifically of the MLX90427.

- **MLX90427 AFE model development** *(28/02 - 18/03)* The Simulink® AFE of the MLX90427 was developed. The AFE model of a previous Triaxis® sensor, the MLX90377, was used as a baseline. Each block of the model was tested. The model was then compiled, exported and validated.

- **MLX90427 integration in the THIL environment** *(21/03 - 22/04)* The exported AFE model of the MLX90427 was introduced in the THIL environment. A long debugging process was necessary before receiving the first meaningful SPI response from the sensor. Many NVRAM parameters had to be adjusted to configure the computations performed by the digital controller, when interfaced with the AFE model. For instance, the temperature computation had to be adapted to the linear temperature sensor model, which was implemented. Also, the supply voltage system diagnostics had to be disabled because it is neglected in the AFE model.

- **Kostal workshop** *(02/05 - 04/05)* The target customer of the MLX90427, was interested in using the THIL to start developing their steering angle sensor before Melexis delivers the final product. A workshop was thus organized for the delivery of a THIL working setup, in the headquarters of the company. I was in charge of preparing a demo of how to use the platform (setting the inputs, executing the model, sending and receiving SPI frames). Being part of this event was a very nice opportunity. Among other things, it allowed me to discover the matters at stake between supplier and customer when developing a complex product.

- **MLX90427 software qualification test platform development** *(05/05 - 17/06)* The goal was to develop a structured and easy-to-use environment for the software qualification tests of the MLX90427. The Robot Framework® was chosen as a user-friendly platform: the test case implementation with human-readable keywords is very intuitive and the test results are easily accessible from the automatically generated log files. Python modules were added to automate the control of the THIL environment.

- **On-site visit of Laurent Fesquet** *(03/06)* My school tutor, Laurent Fesquet, took the time for a visit on-site, in Bevaix, Switzerland. After a discussion with Benjamin Colle, who is my internship supervisor, and Zsombor Lázár, who is the THIL project manager, we went through the objectives of my work at Melexis. He was also able to provide me valuable advice on the redaction of this report.

- **MLX90427 software qualification test integration in the CI process** *(20/06 - 01/07)* As a proof of concept, the THIL was integrated in the Gitlab® CI process of an isolated project, with files manually copied from the MLX90427 software repository. The next step will be to integrate it in the actual SWCC process, to automate the regression tests of the software.

- **THIL workshop for MLX90427 validation** *(04/07 - 07/07)* It was decided that application engineers would use the THIL as a debugging tool in the early stages of the software development. It

allowed the discovery of multiple bugs and considerably sped up the validation of the MLX90427. A workshop was organized on-site to show the application engineers how to use the platform. I was in charge of presenting them the different tools required for the tests.

— **Report redaction** *(09/05 - 05/08)*

— **Oral presentation preparation** *(08/08 - 12/08)*

Figure 26: Delivery of a THIL working setup to the main customer of the MLX90427, 03/05/2022
Jérémie Chabloz (System Architect of the MLX90427), Zsombor Lázár (System Architect and THIL project manager), me, Sébastien Leroy (Functional Safety Architect), two Software Engineers from the company for which the MLX90427 was developed

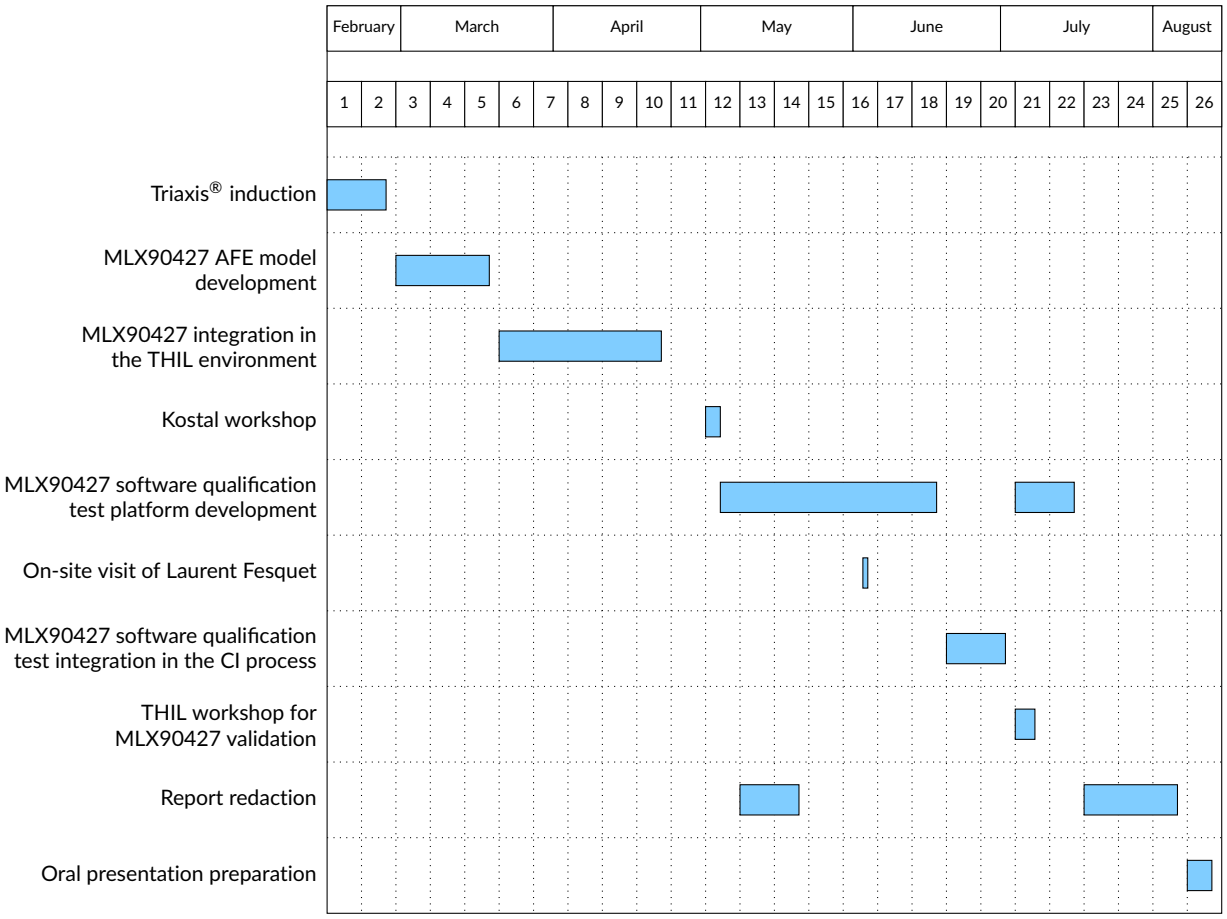

Figure 27: Gantt diagram

References

[1] *Melexis website*. url: https://www.melexis.com/en.

[2] Melexis. *Annual report 2021*. url: https://www.melexis.com/en/investors/results-and-presentations/financial-reports/annual-report-detail-2021.

[3] *Electronics Tutorials*. url: www.electronics-tutorials.ws.

[4] Winncy Y. Du. *Resistive, Capacitive, Inductive, and Magnetic Sensor Technologies*. Ed. by CRC Press. Series in sensors. Dec. 2014.

[5] Olivier Fiat. *Physique - Méthodes et exercices*. Dunod, 2017.

[6] Samuel Huber et al. "A Gradiometric Magnetic Sensor System for Stray-Field-Immune Rotary Position Sensing in Harsh Environment". In: *Proceedings* 2 (Dec. 2018), p. 809. doi: 10.3390/proceedings2130809.

[7] Erich Zabler. *Method and device for angular measurement of a rotatable body*. US patent n°US5930905A. Aug. 1999. url: https://patents.google.com/patent/US5930905/en14.

[8] Jim A. Ledin. "Hardware-in-the-Loop Simulation". In: *Embedded Systems Programming* (Feb. 1999), pp. 42–60.

[9] MathWorks®. *Basics of Hardware-In-The-Loop simulation*. Apr. 2022. url: https://ch.mathworks.com/help/physmod/simscape/ug/what-is-hardware-in-the-loop-simulation.html.

[10] International Organization for Standardization. *Part 6: Road vehicles — Functional safety — Product development at the software level*. Tech. rep. ISO 26262-6:2018. https://www.iso.org/standard/68388.html, 2018.

[11] VDA QMC Working Group 13 / Automotive SIG. "Automotive SPICE Process Assessment / Reference Model". In: Version 3.1 (Nov. 2017). url: https://www.automotivespice.com/.

[12] GitLab. *CI/CD concepts*. url: https://docs.gitlab.com/ee/ci/introduction/index.html#continuous-integration.

A Analog front-end model of the MLX90427

A.1 Analog front-end model parameters

The following parameters were taken from the MLX90427 specifications:

K_T	$3.90\ mV.K^{-1}$
K_S	$-1.75 \times 10^{-2}\ GPa^{-1}$
V_{DD}	$3.3\ V$
V_{bias}	$2.75\ V$
$S_{mismatch}$	0
S_{abs}	0.07
S_{rel}	$-5.5 \times 10^{-3}\ T^{-1}$
S_{rel^2}	$1 \times 10^{-5}\ T^{-2}$
$T_{nominal}$	$35°C$

A.2 Screenshots of the Simulink® model

The inputs and outputs of the model are implemented as ports. The stimuli (angle, temperature and offsets for the diagnostics) are implemented as *global signals* because they can change while the model is being executed. A version control was also implemented.

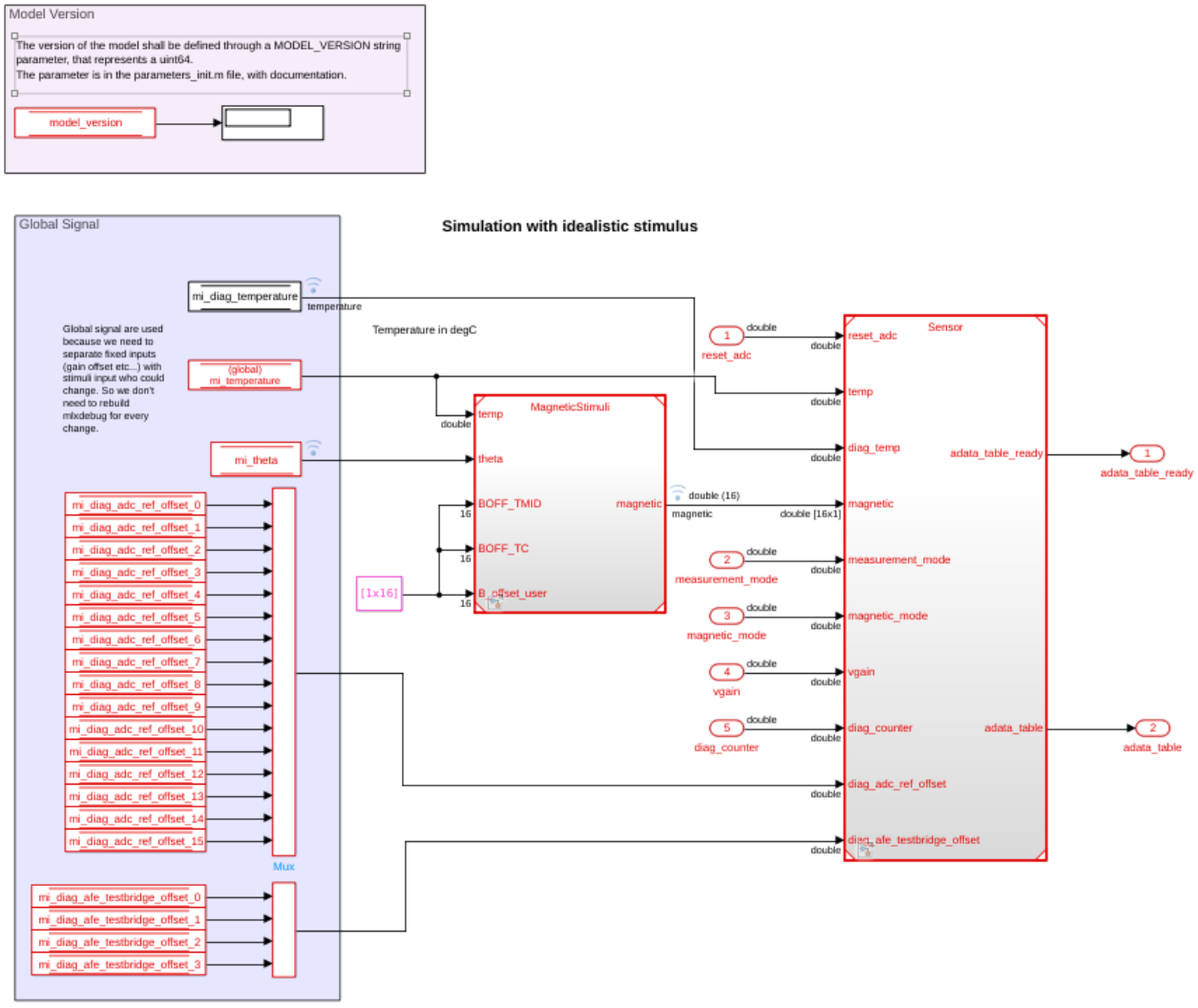

Figure 28: Overview of the Simulink® model

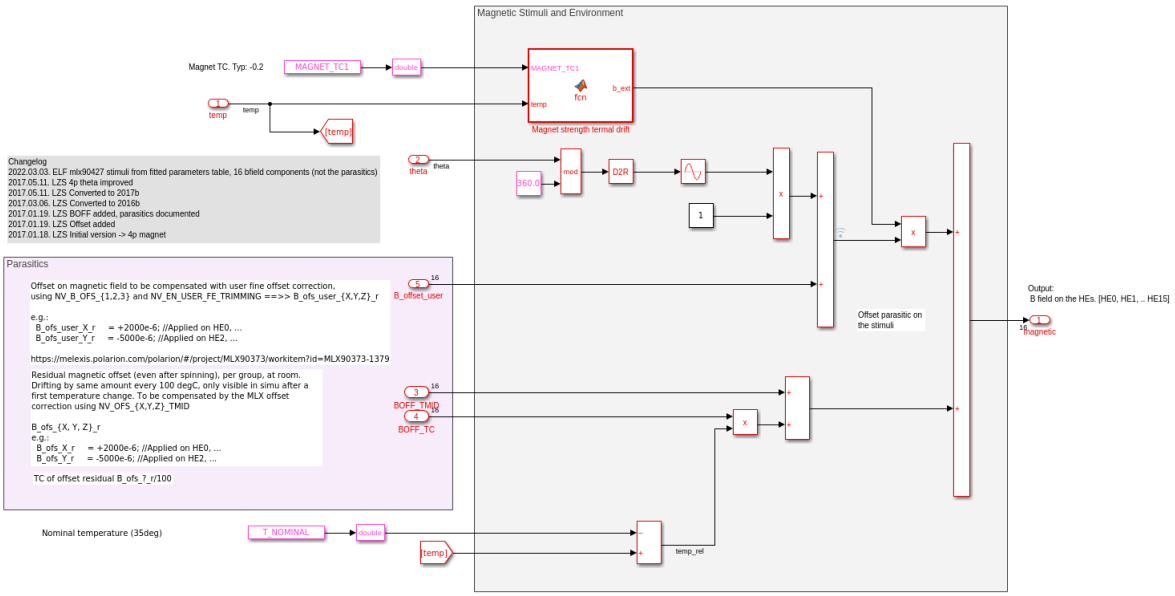

Figure 29: Magnetic stimuli model

Remark. *The magnetic stimuli can be tuned with offsets. These offsets were set to zero within the framework of my study.*

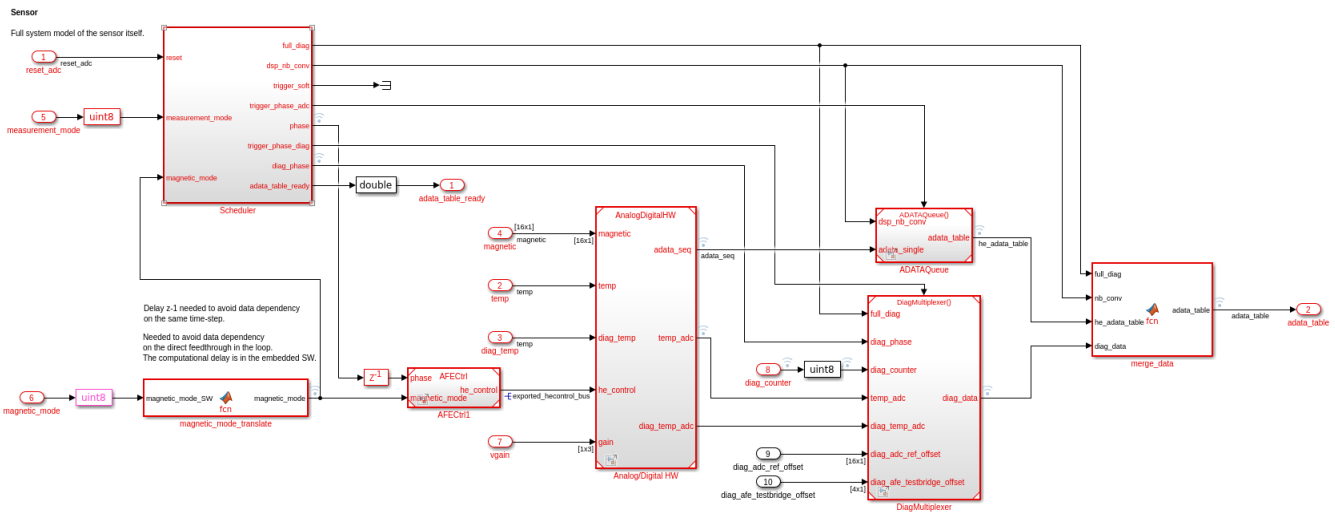

Figure 30: Overview of the analog front-end model of the MLX90427

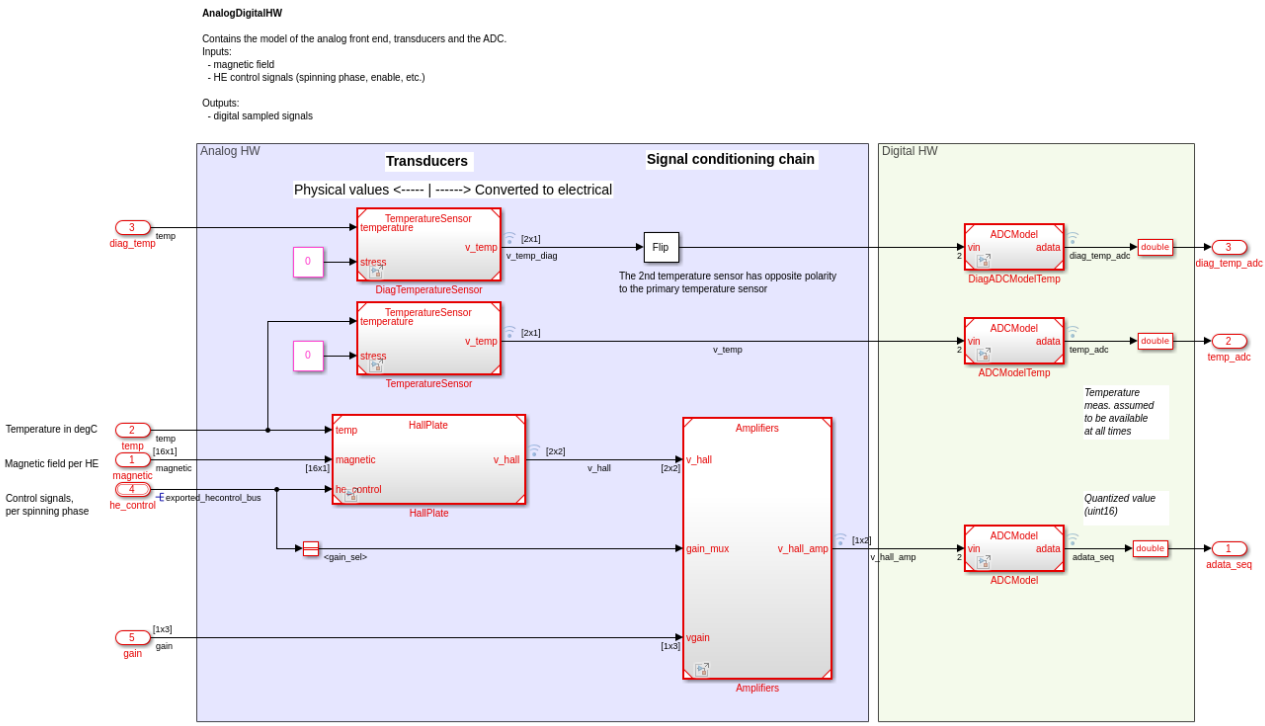

Figure 31: Model of the analog and digital hardware of the MLX90427 analog front-end

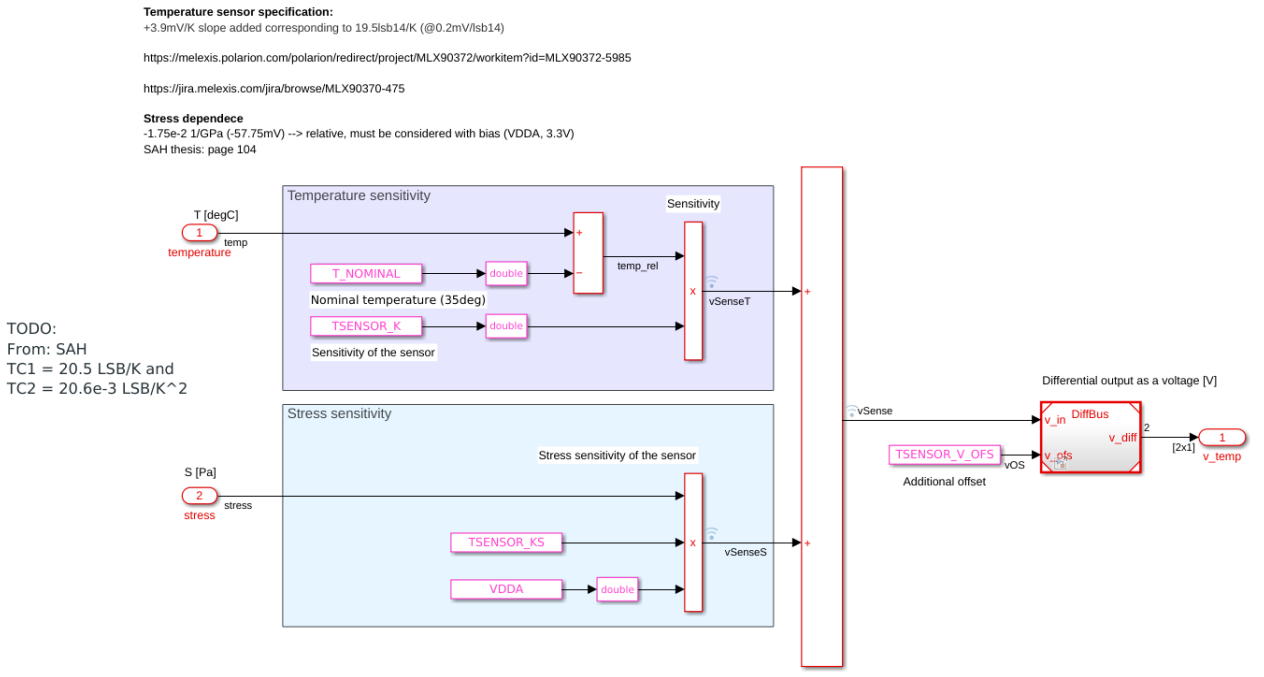

Figure 32: Temperature sensor model

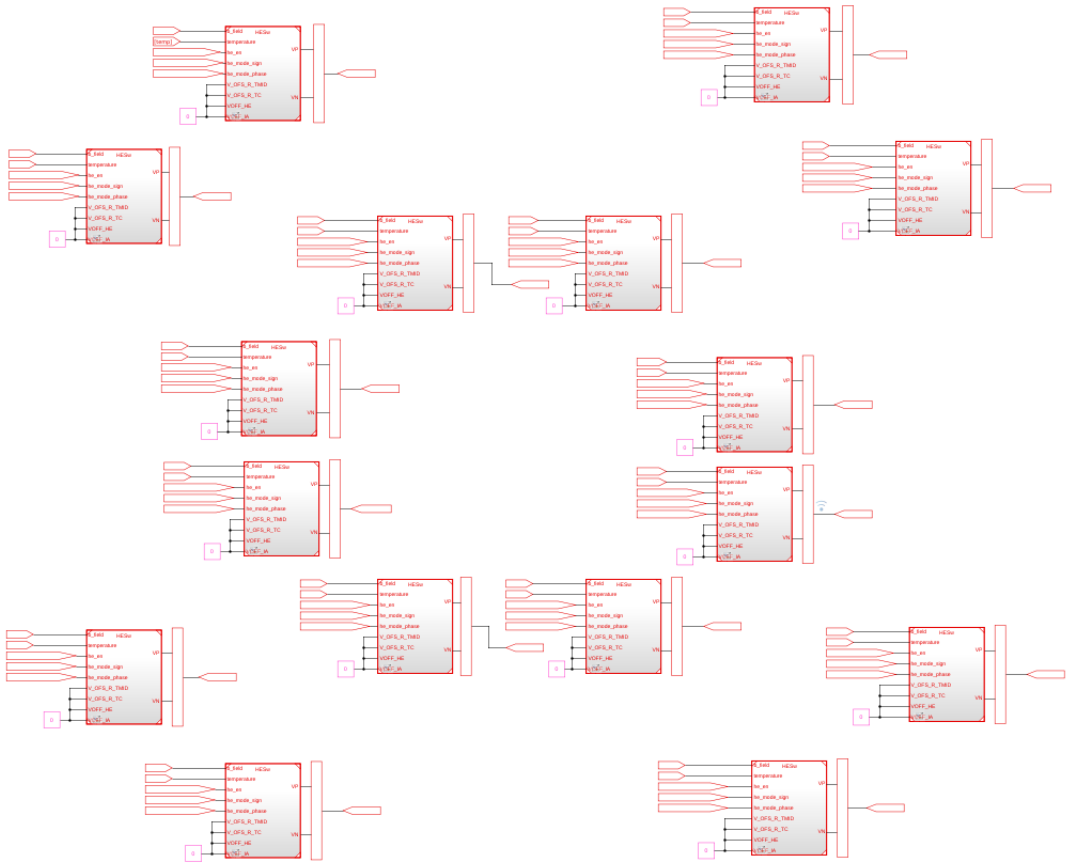

Figure 33: Model of the Hall plates configuration

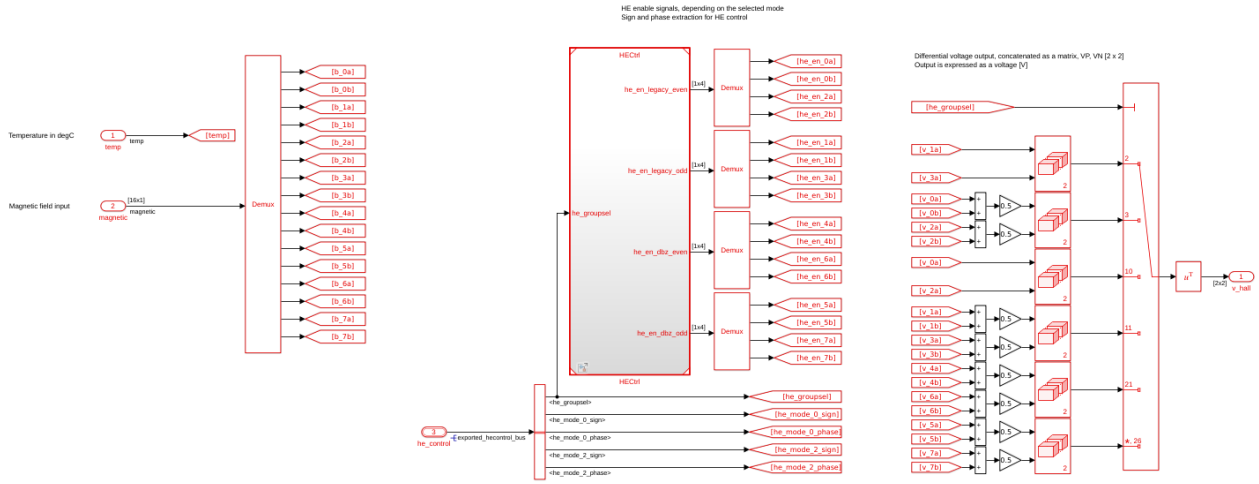

Figure 34: Extraction of the control signals for the Hall plates

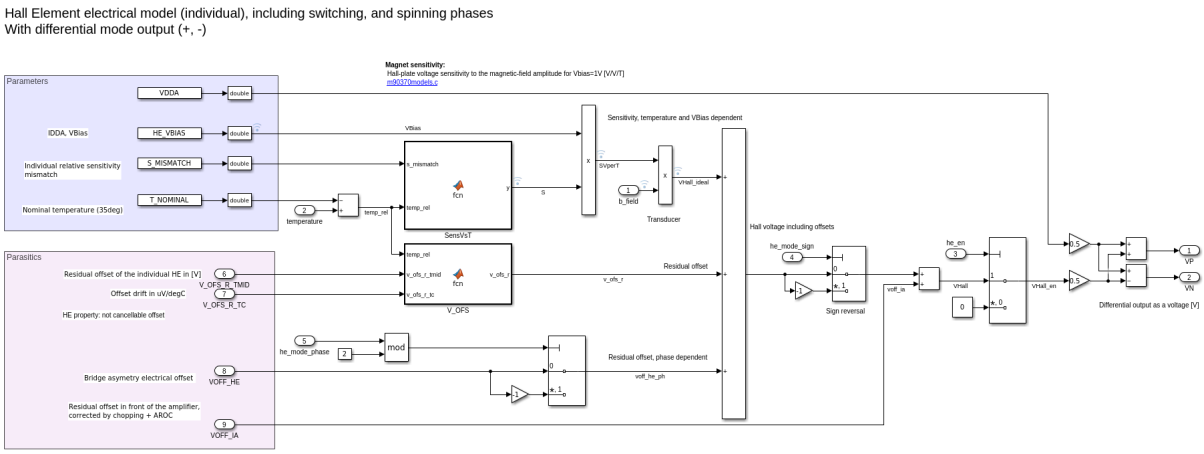

Figure 35: Model of a Hall plate

Remark. *The output of each Hall plate can be tuned with offsets. These offsets were set to zero within the framework of my study.*

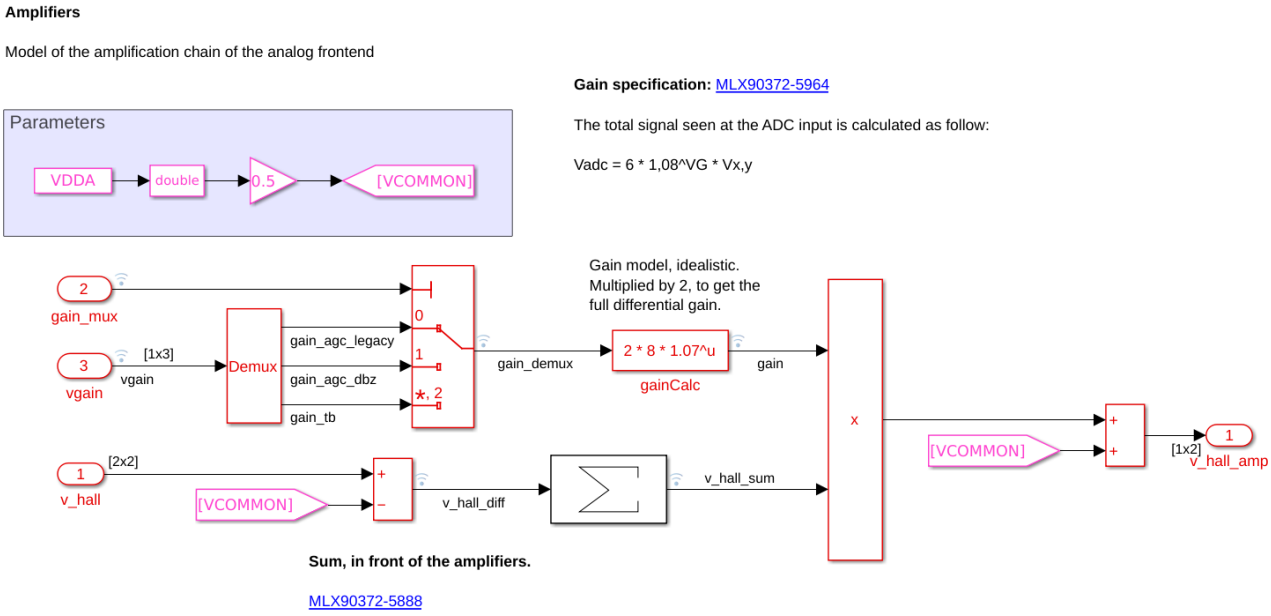

Figure 36: Model of the amplification chain

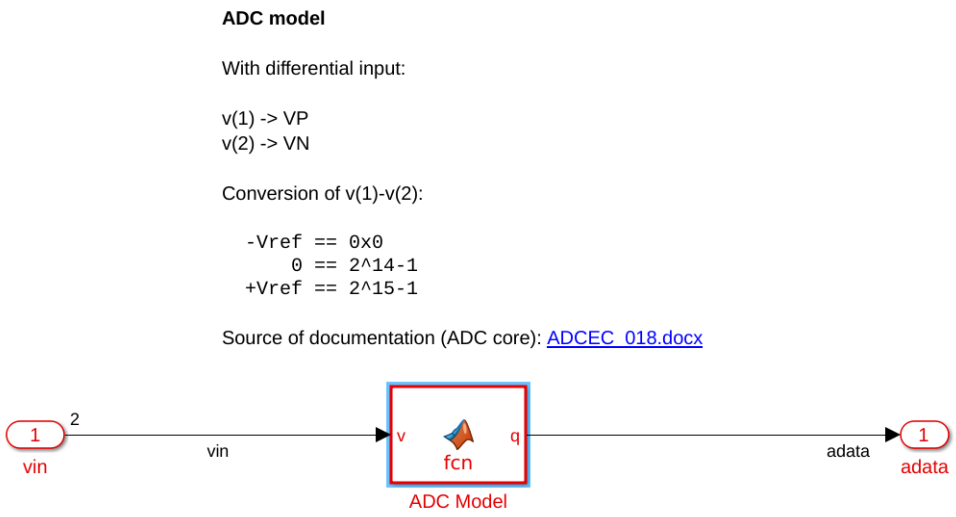

Figure 37: Model of the analog-to-digital converter

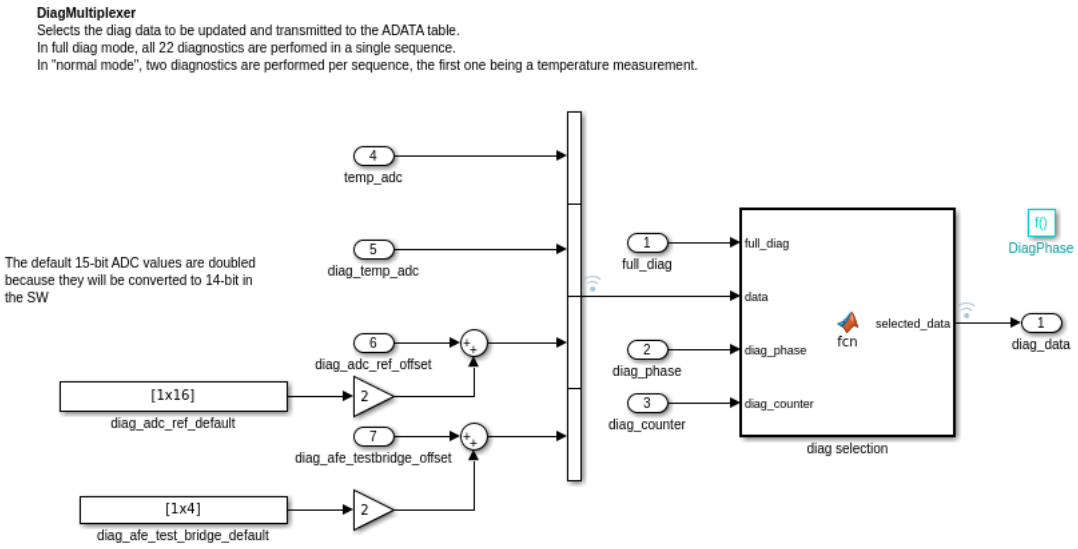

Figure 38: Model of the diagnostics ADATA multiplexer

B Output plots

The results of the angle and temperature measurements were extracted from the SPI return messages received from the MLX90427 emulated by the THIL. They appear to be very close to the expected results, which are the inputs of the AFE model.

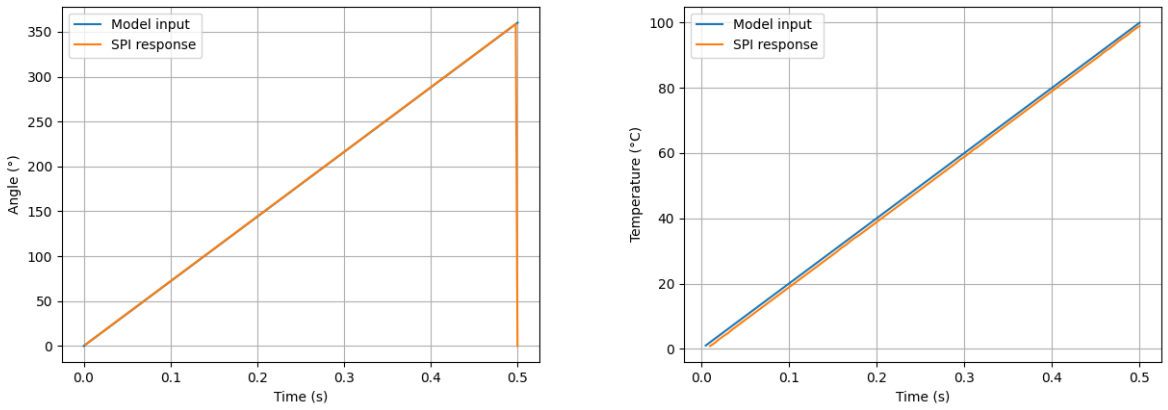

(a) Angular position of the magnet

(b) Temperature measured by the first temperature sensor

Figure 39: Angle and temperature in *Rotary XY* mode

Abstract (EN)

System-level testing is an expensive step of the development process of a product with embedded computing. In particular, the software qualification step comes towards the end of the development process, and consists in verifying that the software fulfills its requirements. Reaching a thorough test coverage, while minimizing the time-to-market and the testing cost has become paramount, especially in safety-critical products used in the automotive industry. The MLX90427 is a smart Hall effect position sensor aimed at the measurement of a vehicle steering angle. A Hardware-In-the-Loop simulation environment was successfully developed for a low-cost, real-time and automated qualification of its ROM-embedded software. To this end, a FPGA-emulation of the digital controller of the sensor was interfaced with an analog front-end model, for the simulation of the magnetic and diagnostic measurements performed by the sensor. The hardware-in-the-loop environment was then automated for an easy regression testing of the MLX90427 software after each update, through a continuous integration process. Thanks to the platform, multiple bugs were successfully detected and rapidly corrected. This participated to the development of a high quality product, within the tight development schedule demanded by the customer.

Résumé (FR)

Lors du développement d'un produit avec logiciel embarqué, les tests systèmes sont une étape couteuse. En particulier, l'étape de qualification du logiciel intervient vers la fin du processus de développement, et consiste à vérifier que le logiciel remplit ses exigences. Pour les produits utilisés dans l'industrie automobile, critiques en matière de sécurité, il est primordial d'augmenter le nombre de tests effectués tout en minimisant leur coût et les délais de commercialisation. Le MLX90427 est un capteur de position à effet Hall, destiné à la mesure de l'angle de braquage d'un véhicule. Pour une qualification automatisée, en temps réel et à faible coût du logiciel intégré dans sa ROM, un environnement de simulation Hardware-In-the-Loop a été développé. Pour ce faire, une émulation sur FPGA du microcontrôleur du capteur a été interfacée avec un modèle Simulink® de son circuit analogique, pour la simulation des mesures magnétiques et de diagnostics effectuées par le capteur. L'environnement hardware-in-the-loop a ensuite été automatisé afin de faciliter les tests de régression du logiciel du MLX90427 après chaque modification, dans le cadre d'un processus d'intégration continue. Grâce à la plateforme, plusieurs défauts logiciels ont été détectés avec succès et rapidement corrigés, ce qui a participé au développement d'un produit de haute qualité, dans les délais exigés par le client.

Abstract (IT)

Il collaudo a livello di sistema è una fase onerosa del processo di sviluppo di un prodotto dotato di elaborazione incorporata. In particolare, la fase di qualificazione del software arriva verso la fine del processo di sviluppo e consiste nel verificare che il software soddisfi i requisiti. Raggiungere una copertura di test completa, riducendo al minimo il time-to-market e i costi di collaudo, è diventato fondamentale,

soprattutto nei prodotti critici per la sicurezza utilizzati nell'industria automobilistica. L'MLX90427 è un sensore di posizione intelligente a effetto Hall per la misurazione dell'angolo di sterzata di un veicolo. È stato sviluppato con successo un ambiente di simulazione Hardware-In-the-Loop per una qualificazione a basso costo, in tempo reale e automatizzata del suo software integrato nella ROM. A tal fine, un'emulazione FPGA del controllore digitale del sensore è stata interfacciata con un modello di front-end analogico, per la simulazione delle misure magnetiche e diagnostiche eseguite dal sensore. L'ambiente hardware-in-the-loop è stato poi automatizzato per un facile test di regressione del software MLX90427 dopo ogni aggiornamento, attraverso un processo di integrazione continua. Grazie alla piattaforma, sono stati individuati e corretti rapidamente numerosi bug. Ciò ha contribuito allo sviluppo di un prodotto di alta qualità, nel rispetto dei tempi stretti di sviluppo richiesti dal cliente.